Band 36 (2000), S. 119–150

ZEITSCHRIFT FÜR
GLETSCHERKUNDE
UND GLAZIALGEOLOGIE

MODELLING MELTWATER PRODUCTION WITH A DISTRIBUTED ENERGY BALANCE METHOD AND RUNOFF USING A LINEAR RESERVOIR APPROACH – RESULTS FROM VERNAGTFERNER, OETZTAL ALPS, FOR THE ABLATION SEASONS 1992 TO 1995*

By H. ESCHER-VETTER, Munich

With 13 figures

ABSTRACT

A distributed energy balance meltwater production model, designed and applied in the 1980's for the Vernagtferner basin, Oetztal Alps, Austria, has been further developed and tested with data from the ablation seasons 1992 to 1995. It starts from meteorological and hydrological records and empirical functions at one site and expands these data on the basis of the 100 m digital terrain model. Thus, air temperature, precipitation, surface temperature and ground heat flux are regionalized and parameterised, respectively, and turbulent fluxes are determined with a bulk approach. The global radiation distribution modelling takes into account terrain dependent effects, and the ageing of the snow cover from newly fallen snow to very dark firn is implemented in the modelling of radiation absorption. Whereas the absorptivity for ice (0.6) is pre-set externally, values of 0.3 or 0.2 for newly fallen snow are deduced from sensitivity tests. The model results show a good agreement with data such as (1) the altitudinal mass balance profile, (2) the overall size of the ice area and (3) its temporal-spatial development. For three hydrological different areas, the resulting runoff components are modelled with a linear reservoir approach, testing different recession coefficients for each reservoir. The runoff model performance is discussed on a statistical basis and by the comparison of time series of discharge. The total difference between modelled and recorded discharge amounts to 7 % in 1992, 9 % in 1993 and 5 % in 1995.

MODELLIERUNG DER SCHMELZWASSERPRODUKTION MIT EINEM ENERGIEBILANZ-ANSATZ UND DES ABFLUSSES MIT EINEM LINEAREN SPEICHERMODELL – ERGEBNISSE FÜR DIE ABLATIONSPERIODEN 1992 BIS 1995 AM VERNAGTFERNER, ÖTZTALER ALPEN

ZUSAMMENFASSUNG

In dieser Arbeit wird die Erweiterung eines Energiebilanz-Schmelzwasserproduktionsmodells beschrieben, das in den achtziger Jahren für den Vernagtferner, Ötztaler Alpen, entwickelt wurde. Es basiert auf meteorologischen und hydrologischen Messreihen und empirischen Funktionen von einem Punkt des Einzugsgebietes und deren räumlicher Extrapolation auf der Basis eines digitalen Geländemodells mit 100 m Maschenweite. Dabei werden Lufttemperatur, Niederschlag, Oberflächentemperatur und Bodenwärmestrom regionalisiert bzw. parametrisiert, die turbulenten Flüsse mit einem Bulkansatz modelliert. Bei der Globalstrahlungsverteilungsmodellierung werden Geländefaktoren berücksichtigt, und das Altern der Schneedecke von Neuschnee zu sehr dunklem Firn wird in die Strahlungsabsorptionsmodellierung eingebracht. Der Absorptionswert für Eis (0.6) wird extern vorgegeben, die Werte für Neuschnee (0.3 bzw. 0.2) mit Hilfe von Sensitivitätsanalysen abgeleitet. Die Modellergebnisse zeigen eine sehr befriedi-

* Contribution no. 1 of the working group of glaciology GLOWA-DANUBE

gende Übereinstimmung mit (1) der Höhenverteilung der Massenbilanz, (2) der Gesamtgröße des Eisgebietes und (3) seiner zeitlich-räumlichen Entwicklung. Für drei hydrologisch unterschiedliche Teilgebiete des Gletschers werden die resultierenden Abflusskomponenten mit einem Linearspeicheransatz berechnet, wobei mehrere Kombinationen von Abklingkonstanten für jedes Teilgebiet untersucht werden. Die Güte des Abflussmodells wird an Hand statistischer Daten und durch Zeitreihenvergleiche gezeigt. Der Unterschied zwischen modellierten und registrierten Gesamtabflüssen liegt bei 7 % (1992), 9 % (1993) und 5 % (1995).

1. INTRODUCTION

Vernagtferner in the Oetztal Alps is a glacier with a period of observation starting in the 17th century. The first map of the glacier at 1 : 10,000 was prepared by Sebastian Finsterwalder in 1889 (Finsterwalder, 1897). Direct mass balance measurements were started in 1964 (Reinwarth and Rentsch, 1994). Since then, the glacier behaviour has been monitored photogrammetrically on a time scale of tens of years and glaciologically annually. The construction of a permanent station about 1 km downstream from the glacier terminus, the so-called "Pegelstation Vernagtbach", in 1973 (Bergmann and Reinwarth, 1976) provided the means of monitoring a basic set of meteorological and hydrological variables with a high temporal resolution (days to hours). With this data set it became possible to force a distributed energy balance as well as a runoff model of Vernagtferner. Repeated photogrammetric surveys of the glacier – using terrestrial and aerial photogrammetry – and the determination of the mass balance of Vernagtferner with the direct glaciological method were continued.

A combined meteorological-hydrological-glaciological investigation program (Moser et al., 1986) was carried out in the drainage basin of Vernagtferner (Fig. 1) from 1974 to 1986. During this program, the meltwater production and runoff models were first designed (e.g. Baker et al., 1982, Escher-Vetter, 1985, Moser et al., 1986), based on a Digital Terrain Model (DTM) of the glacier of 1969 with a grid width of 100 m. The DTM, used in the actual study, is based on an orthophoto of Vernagtferner from 1990 (Heipke et al., 1994). The major part of the present paper concentrates on the further development of the original meltwater production model and its validation by independently determined variables, such as the mass balance or the temporal-spatial development of bare ice area. In a second, shorter part, the performance of the runoff model is discussed in terms of statistical numbers and of time series of modelled and recorded discharge. The calculations were performed for the ablation seasons 1992 to 1995, which consist of two moderately negative (1993, 1995) and two strongly negative (1992, 1994) balance years.

There are not many glaciers – if any – whose behaviour is monitored on all these time scales, i.e. from decades down to hours. Therefore, the development, application and validation of a – although simple – physical meltwater production model in combination with a runoff model on such a glacier deliver the tools to transfer it to other regions, to use it, for example, for runoff modelling in regions without discharge records. The modular design makes it possible to exchange some parameterizations, if necessary or desirable. Thus, the shrinkage of the glaciers in the Zugspitz region, Bavaria, was studied with the Vernagtferner energy balance model (Arck and Escher-Vetter, 1997), using daily data from the weather station at Zugspitze instead of hourly ones as in this study. Mader and Kaser (1994), on the other hand, applied the same concepts and even the same hydrological parameters to modelling of a distinctly different glacierized region in Austria (Ochsental, Silvretta), resulting in a very good agreement between modelled and measured discharge. Arnold et al. (1996) used some of the basic concepts of the Vernagtferner energy balance model to study ab-

lation on Haut Glacier d'Arolla, Switzerland. They applied a grid width of 20 m for a rather similar modelling of the energy balance terms as in this study, and they also used the concept of Escher-Vetter (1980) in calculating the aspect and the slope for each pixel of their investigation area. The high spatial resolution of 20 m certainly offers some advantage for the evaluation of the incoming solar radiation, when the terrain is rather rugged, with steep slopes and large shading effects of surrounding mountains. For the parameterisation of the turbulent fluxes with a bulk approach, however, it might worsen the results. From the typical recording height of 2 m for temperature, humidity and wind speed, a horizontal averaging length for the flux determination results in the order of 100 m to 300 m upwind. That means that the fluxes are representative for areas of several thousand square meters, but not for smaller areas. But as the turbulent fluxes only play a smaller part in the complete melting process, and due to a rather accurate modelling of the surface albedo, the model output for Haut Glacier d'Arolla agreed rather well with the snow-line retreat, the albedo, and the ablation, as they were observed for June and July 1990.

Another study (Hofinger and Kuhn, 1996) concentrated on the evaluation of summer mass balances of Hintereisferner, Oetztal Alps, by applying an energy balance model which is driven by the climate data of the Vent station, in a distance of approximately 10 km from the glacier snout. There, the components were determined on a daily basis, with concentration on shortwave radiation balance and albedo, which were internally generated in the model. Monthly temperature gradients were derived for different conditions in cloudiness, and turbulent heat fluxes were calculated with a bulk approach. Model sensitivity tests clearly demonstrated the influences of changes in temperature, and the higher standard deviation of summer compared to winter mass balance confirmed the importance of summer snow falls for annual balance values.

The importance of air temperature distribution is also stressed by Greuell and Böhm (1998). They analysed the lapse rates for the altitudinal range of Pasterze, the largest glacier in Austria, and the implications for the sensitivity of the mass balance. Oerlemans and Knap (1998), on the other hand, discuss a rather detailed albedo scheme for use in mass balance modelling, derived from data on Morteratschgletscher, Switzerland. An optimization of five control parameters reproduces the observations reasonably well, if snowfall events and snow depth are used as input, which means that these data have to be provided externally.

The probably most detailed overview of current meltwater production models is given in the doctoral thesis of Hock (1998). Based on extensive field data from Storglaciären, Sweden, simple parameterisations as for example degree-day approaches are discussed as well as fully developed energy balance models. Various kinds of sophistication are implemented, partly based on the schemes developed for Vernagtferner. On a whole, the model performance increased, when more detailed approaches were applied: (1) The inclusion of a radiation index into a distributed temperature index model catches the daily discharge cycles better than the classical degree-day method. (2) A separation of the radiation components into direct, diffuse, longwave sky and longwave terrain components, considering topographic effects, delivers better results than calculations only with global radiation and constant longwave radiation (Hock and Noetzli, 1996). (3) Internal generation of albedo is superior to external prescription of this most important quantity.

In the study presented in the following, those results and concepts from the above mentioned investigations were incorporated in the **P**hysical **E**nergy balance model of **V**ernagtferner PEV, which were considered to be applicable in the modelling of the meltwater production of this glacier.

2. MELTWATER PRODUCTION

2.1 ENERGY BALANCE EQUATION

The core of the meltwater production model consists of an energy balance approach (Escher-Vetter, 1985). A quite simple parameterisation of the individual terms is used when only a minimum set of input data is available. The model delivers the available melt energy, M, in W m^{-2}, as the sum of shortwave and longwave radiation balance (RS and RL, respectively), sensible (H) and latent (LE) heat fluxes, and ground heat flux (B), all in W m^{-2}, thus:

$$RS + RL + H + LE + B = -M \quad (1)$$

$$G(1-a) + L\downarrow_{cl} - \sigma(T_S + 273.16)^4 + \alpha(T - T_S) + \alpha(0.623r/(p\,c_p))(e - E_{Ts}) + B = -M \quad (1a)$$

where

G	global radiation	W m^{-2}
a	albedo	
$L\downarrow_{cl}$	longwave radiation of the atmosphere	W m^{-2}
T_S	surface temperature	°C
T	air temperature	°C
p	pair pressure	hPa
e	water vapour partial pressure (air)	hPa
E	water vapour saturation pressure (surface)	hPa
α	heat transfer coefficient	W m^{-2} K^{-1}
σ	Stefan-Boltzmann constant	W m^{-2} K^{-4}
r	heat of fusion	J kg^{-1}
c_p	specific heat of the air	J kg^{-1} K^{-1}

All terms are positive, when energy is transferred to the surface, thus, melting is designated by a negative sign on M.

2.1.1 MEASURED AND EMPIRICALLY DERIVED INPUT DATA AT ONE SITE

For the site of the Pegelstation Vernagtbach (2640 m a.s.l.), the measured as well as the empirically derived model input data are summarized in Table 1. All records comprise hourly averages with the only exception of precipitation, which is monitored on a daily basis. The same applies for daily averages of cloud cover, the snow line altitude and the Bolz coefficient, discussed later.

Table 1: Model input data, directly recorded or empirically derived for the site of the Pegelstation Vernagtbach

Recorded	Symbol	Unit	Empirical	Symbol	Unit
Global radiation	G	[W m^{-2}]	Albedo	a	–
Air temperature	T	[°C]	Surface temperature	Ts	[°C]
Relative humidity	f	[%]	Longwave incoming radiation	$L\downarrow_{Cl}$	[W m^{-2}]
Wind velocity	v	[m/s]	Heat transfer coefficient	α	[W m^{-2} K^{-1}]
Air pressure	p	[hPa]			
Discharge	Q	[m^3 s^{-1}]			
Precipitation	P	[mm]	Bolz coefficient	B_c	–
			Snow line altitude	–	m a.s.l.
			Cloud cover	*cl*	–

The most important quantity for meltwater production modelling, which is not directly monitored, is the shortwave albedo of the glacier surface. A nearly exponential decay of snow albedo with time was observed, among others, by US Army Corps of Engineers (1956) and Wagner (1979) and was incorporated into energy balance models by Rohrer (1992) and Hofinger and Kuhn (1996). Setting absorptivity $b = (1 - a)$ and rewriting Rohrer's relationship for b, it becomes

$$b = b_h - (b_h - b_l) \exp(-n\,i) \tag{2}$$

where

b is the actual absorption value of snow, subscripts *h* and *l* refer to the highest and lowest absorption value of snow,

n is the number of days since the last "significant" snowfall, and

i is a scaling factor.

For sites with temperature recordings, Rohrer uses $i = 0.12$ when mean daily air temperature is higher than 0 °C, and 0.05 otherwise. In this study, a value of 0.12 was used throughout the summer and for the entire snow-covered portion of the glacier area. "Significant" snowfall was assumed to be more than 1 mm w.e. per day, which is comparable to the value of 3 cm snowfall in 3 days used by Rohrer. This value reflects the low precipitation amounts in the region of Vernagtferner, typical for the Inner Oetztal which represents a rather dry central alpine valley (Fliri, 1975).

The actual numbers of b_h and b_l were determined as follows: At the beginning of the ablation season, the shortwave radiation absorption, as recorded at the site of the Pegelstation Vernagtbach, varies between 0.2 and 0.3 for different years. From sensitivity tests with total mass balance (c.f. Table 3), 0.2 proved to be the better choice for the years 1992 and 1995, 0.3 for 1993 and 1994. In order not to incorporate too many externally prescribed different values for absorption, newly fallen snow in summer was attributed with the same value. The highest absorption value for firn, i.e. b_h, was set to 0.59, and the shortwave absorption coefficient of ice is kept constant at a value of 0.6 throughout the modelling period.

If there is no energy available for melt (i.e. $M < 0$), surface temperature T_S is determined using a formula derived from the heat transfer equation (e.g. Ambach 1955, Brunt 1944).

$$T_S = 2\,M\,(t/(\pi\,k\,\varrho\,c))^{0.5}, \tag{3}$$

where T_S is in °C, when M is given in W m^{-2} and t in seconds. The product of thermal conductivity k, density ϱ, and specific heat c equals 48.3 * 10^5 W^2 s m^{-4} K^{-2} in the case of ice and 24.6 * 10^5 W^2 s m^{-4} K^{-2} for snow and firn of density 800 kg m^{-3}. For example: when the energy loss M amounts to -100 W m^{-2} for a time span $t = 300$ s, the surface temperature is reduced from 0 °C to -0.9 °C at the ice surface, but to -1.3 °C, when there is firn or snow at the surface. This approach does not take into account the freezing of water in the snow or firn.

Long-wave incoming radiation under cloudless conditions, $L\downarrow_0$, is determined by an empirical approach of Brunt (1932), which uses air temperature and relative humidity for parameterization of $L\downarrow_0$ according to

$$L\downarrow_0 = \sigma\,(T + 273.16)^4\,(0.610 + 0.050\,e^{0.5}). \tag{4}$$

$L\downarrow_0$ is in W m^{-2}, when T is in °C and e is in hPa. The Stefan-Boltzmann constant σ equals 5.67 * 10^{-8} W m^{-2} K^{-4}.

For the determination of the actual long-wave incoming radiation, $L\downarrow_{cl}$, cloud cover cl is determined as the ratio of the global radiation, as recorded at the Pegelstation Vernagtbach, to the global radiation on cloud-free days, as given by Tables of Sauberer and Dirmhirn (1958). Knowing cl for every day, then, $L\downarrow_{cl}$ is determined by

$$L\downarrow_{cl} = L\downarrow_0 (1 + B_c (cl)^2) \tag{5}$$

(Geiger, 1961), where B_c is an empirical coefficient derived by Bolz (1949). In this study, B_c is set to fixed values for fixed cloud cover ranges (Table 2). For days with precipitation, B_c was set to 0.24. As cloud cover is determined on a daily basis, so is B_c.

Table 2: Dependence of B_c from cloud cover for days without precipitation

Cloud cover	0–0.2	0.2–0.6	0.6–1.0
B_c	0.08	0.17	0.20

Perhaps the crudest empirical equation is that used for the determination of the heat transfer coefficient α (Escher-Vetter, 1980). As the data set at the Pegelstation Vernagtbach does not include wind profile recordings, a gradient approach could not be used. Therefore, Equation (6) is based on wind velocity records in a single height, it delivers α in W m^{-2} K^{-1}, when v is in m/s, according to

$$\alpha = 5.7 * v^{0.5}. \tag{6}$$

This relation is based on evaporation measurements at Weißfluhjoch, Davos, Switzerland, performed by de Quervain (1951), which included wind velocity data measured at 2 m above a snow surface. From these data, Hofmann (1965) derived typical values of α for wind velocities up to several m/s, which can be approximated by Equation (6). Results using these values of α have to be considered with great caution, as the relation implies a uniform roughness length for sensible as well as latent heat flux, and accounts only implicitly for stable stratification over snow and ice. Other studies, e.g. Oerlemans (1993), use a time-independent transfer coefficient, depending only on equilibrium line altitude.

2.1.2 EXPANSION OF INPUT PARAMETERS TO THE ENTIRE GLACIER AREA

Air temperature

Air temperature is the one parameter which influences all the terms of the energy balance, be it directly or indirectly. As continuous recordings are restricted to one site in the drainage basin, suitable assumptions have to be made to get air temperature values for all pixels of the DTM. They are based on (1) short-term measurements of air temperature at a second place and (2) the cloud cover data derived from global radiation recordings (c.f. 2.1.1).

Parallel recordings of air temperature at the Pegelstation Vernagtbach (2640 m a.s.l.) and at the Gletschermitte Station (3078 m a.s.l., c.f. Fig. 1) during the 1970's allowed the determination of diurnally variable lapse rates for three ranges of cloudiness (Fig. 2). They should not be interpreted as vertical gradients of air temperature, but rather as changes of the 2 m-temperature with altitude along the glacier surface. Note the smaller lapse rate during early morning hours when the air above the glacier is warmed earlier than that in the valley, and also the higher amplitude of the variation under cloudless conditions. For rainy days, a constant value of -0.60 K/100 m was used.

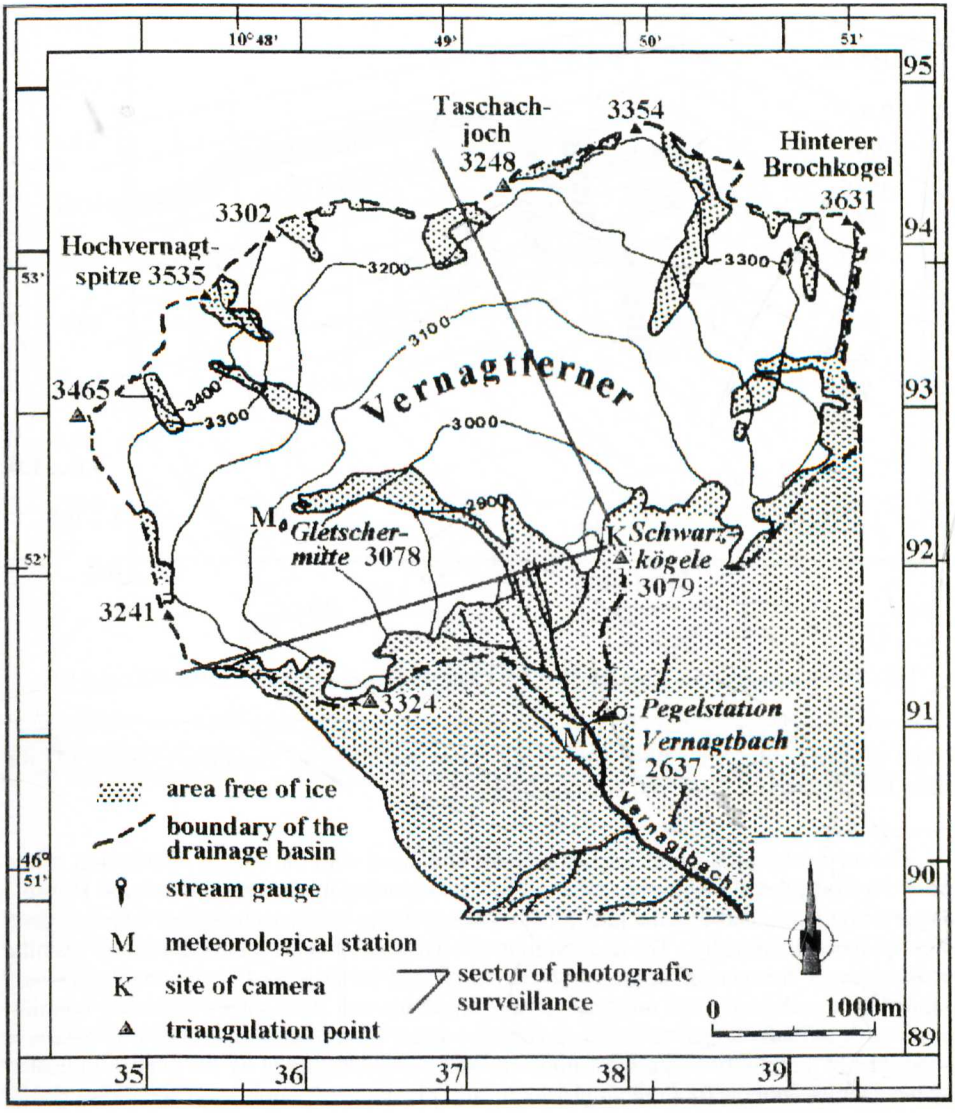

Fig. 1: Map of the drainage basin of the Pegelstation Vernagtbach, Oetztal Alps, Austria (11.44 km^2, 80 % glacierized, 2637 m a.s.l. to 3631 m a.s.l.), showing Vernagtferner and its forefield. The position of the recording sites and the area surveyed by an automatic camera are included in the map.

With this air temperature distribution for the altitudinal range of the glacier, the following quantities are calculated for each pixel of the DTM: (1) the water vapour partial pressure, based on the assumption that relative humidity, as it is recorded at the Pegelstation Vernagtbach, remains constant in the drainage basin, (2) the long-wave incoming radiation,

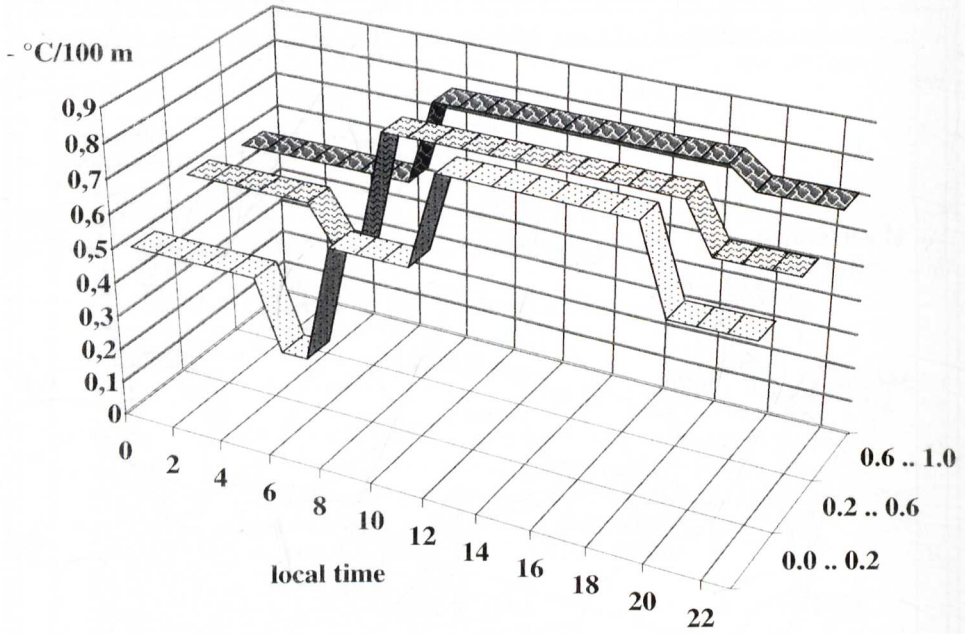

Fig. 2. Diurnal variation of lapse rate for three ranges of cloudiness, $0.0 \leq cl \leq 0.2$, $0.2 < cl \leq 0.6$, $0.6 < cl \leq 1.0$.

based on temperature, humidity and cloud cover according to Equation (5), and (3) the snow line altitude for days with precipitation.

Precipitation

The meltwater production calculations are initialised with the spatial distribution of the water equivalent of the winter snow cover at the beginning of the ablation season. Figure 3 displays the altitudinal distributions for the years 1992 to 1995, interpolated with a second order polynomial function. The distributions of 1992 and 1994 are characterised by maxima in the part of the glacier between 3100 m a.s.l. and 3150 m a.s.l., with maximum w.e. values in the range of 1000 mm to 1150 mm. In 1993 and 1995 values increased continuously with altitude, which is not observed very often on Vernagtferner. There is clearly a good deal of variability in the measurements which is not captured by the curves, indicated by the various symbols for the four years.

During the ablation season, precipitation records are available on a daily basis. Therefore, the snow line, which is approximated by the altitude of the +2 °C-isotherm, is based on the daily average of air temperature. Model precipitation is enlarged by 20 % compared to the records and it is assumed to fall at the beginning of the day.

Global radiation

Although air temperature influences all the energy balance terms, the shortwave radiation balance plays the most important role in meltwater production on alpine glaciers (e.g. Hoinkes, 1955; Braithwaite and Olesen, 1990; Oerlemans, 1993). Therefore, in this study, emphasis is placed on modelling the spatial distribution of global radiation. To do this, the

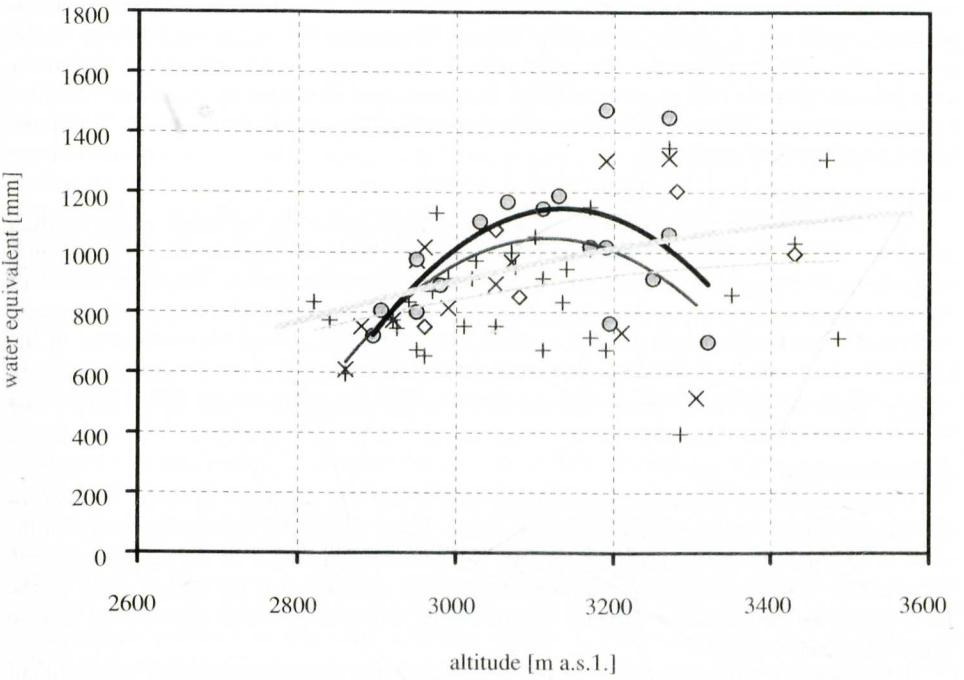

Fig. 3. Variation of specific values of winter snow cover (mm w.e.) with altitude, as surveyed at the beginning of the ablation seasons 1992 (dark thin, symbol x), 1993 (light thin, symbol +), 1994 (dark thick, symbol ○) and 1995 (light thick, symbol ◇); the interpolations are determined as polynomial functions of the measurements.

effect of the steepness and orientation of slopes (internal shading), and shadowing effects of surrounding mountains (external shading) are modelled as described in Escher-Vetter (1980). For Vernagtferner, the slope orientation, average slope angle, and altitude of surrounding mountains are such that these effects are rather small in summer. Therefore, the terrain dependent modification was applied to global radiation instead of direct solar radiation, thus altering sky radiation to the same degree as the direct component. The resulting error is not likely to be significant, particularly since completely sunny days, where these effects play their most dominant role, are rare in such high mountain regions. However, in winter, some steep north-facing slopes of the glacier receive no direct radiation at all, due to this terrain dependence.

Radiation absorption

The spatial distribution of absorption of shortwave radiation is determined as follows: At the beginning of the ablation season, the glacier surface is covered with snow with the absorption coefficient b_l. As long as no snowfall occurs, the absorption increase from this starting value is calculated with the use of eq. (2) for every pixel of the glacier and every time step, until the final value of 0.59 for b_h is reached. When, according to the melt amounts determined by the model, winter snow has melted away, ice appears at the glacier

surface in the region below the firn line of the previous year and the value of 0.6 for the absorption coefficient is attributed to these pixels. When snowfall occurs in any part of the glacier, absorption is reduced to the value of b_l in these areas, for the remaining glacier region it is unchanged. This procedure differs from that used in the earlier model calculations (e.g. Escher-Vetter, 1985), where the temporal as well as the spatial development of absorption were prescribed externally.

Surface temperature

The determination of T_s according to eq. (3) clearly shows the influence of the melting progress. As the quantity M represents the energy loss from the surface during times with no melting, it depends on all the terms of the energy balance equation. The same holds for the constants k, ϱ, and c, as they vary with the surface material. The surface temperature distribution is initialised with a value of 0 °C. Then, eq. (3) is solved for every pixel of the DTM, starting with the snow/firn value of $24.6 * 10^5$ $W^2 s m^{-4} K^{-2}$ for the product of k, ϱ, and c. When, according to the model, no snow is left, the value for ice ($48.3 * 10^5$ $W^2 s m^{-4} K^{-2}$) is used.

Ground heat flux

Ground heat flux, initialised with a value of 0 W m^{-2}, is supposed to be the residual of the energy balance during times without melting. If the cooling of the surface is not sufficient to balance the energy equation, energy losses during the night or during periods with bad weather and no melting are summed up and are compensated by energy gains in the morning or during periods with good weather. Only when these losses are reduced to zero can melting start again.

To complete this short overview of spatially distributed input variables, one should mention that air pressure in eq. 1 is calculated by decreasing the recorded data from the Pegelstation Vernagtbach linearly, using a gradient as defined by the values of the standard atmosphere, and that wind velocity is assumed to have no spatial variation at all.

2.2 RESULTS OF THE ENERGY BALANCE MODEL

2.2.1 SPATIAL AVERAGING OF MODEL OUTPUT

The model runs start after the measurements of the winter snow cover, which were completed on 12 May 1992, 5 May 1993, 1 May 1994, and 22 May 1995, and end on 30 September.

As we are concerned, later, with the modelling of runoff from Vernagtferner, the resulting melt energy M will be discussed in terms of meltwater production. Figures 4a to 4d show average values for every 10 d period, including both meltwater and runoff from rain, if any, for the four years. Subtotals are shown for the ice, firn, and snow areas of the glacier. The names of the averaging areas were chosen according to the state of the surface at the end of the mass balance year, they do not reflect the development of the surface material in the course of the ablation season. – This may be a little bit unusual for hydrologists, but not at all for mass balance specialists. – Thus, "ice" characterises the bare ice area, "firn" stands for that region, where there is no winter snow at the end of the ablation season, exposing firn on the surface. "Snow" is the name for the highest section of the glacier, where winter snow covers firn even to the end of the ablation season. In earlier calculations, the delineation between firn and snow area was taken to the contour 50 m higher than the equilibrium line altitude ELA of the previous year. This was a good approxi-

mation for years with an ELA well below the highest point of the glacier. In the 1990's, however, the ELA was sometimes at the upper margin of Vernagtferner, and sometimes even higher. Therefore, the 3300 m a.s.l. contour line was used as separation between the firn area (in the lower part of the glacier) and the snow area, higher up. Such partitioning implies that at the beginning of the ablation season, only two areas are distinguished, namely the firn area, which corresponds to the region with absorption modelling according to Equation (2), and the snow area, which include 86 % and 14 % of the glacier surface, respectively. After the appearance of bare ice at the glacier surface, the size of the ice region increases at the expense of the firn area, whereas the size of the snow area stays constant during the whole ablation season.

2.2.2 DISCUSSION OF THE MODELLED MELTWATER PRODUCTION FOR THE ABLATION SEASONS 1992 TO 1995

In 1992 (Fig. 4a), the model predicts a rather low meltwater production during May and the beginning of June. Most of the melt is from the firn area. Significant amounts of meltwater from ice areas are modelled only during August. These amounts never reach the values of firn meltwater as modelled for the end of July. As a result the highest total meltwater production of this year falls into the last ten days of July. Model melting is generally low in the snow area. Snowfall at the end of August reduces the model meltwater production in September to values which are more typical for October.

1993 (Fig. 4b) shows a radically different picture: meltwater production is modest over a longer period in the firn area, rather small in the ice area and, again, very low for the snow region, resulting in a broader distribution than in 1992. Maximum model production occurred during the second ten days of August, which is rather late in the season, and therefore amounts to only about 2.90 $m^3 s^{-1}$.

For 1994 (Fig. 4c), the model suggests high production values over a rather long period, resulting in the largest modelled total meltwater amounts of the four years. This year saw the highest discharges since 1974 (Braun and Escher-Vetter, 1996). Although ice appeared at the surface even later than in 1993, the modelled production from this area increased rather quickly, thus contributing to an average total of 5.23 $m^3 s^{-1}$ in the first ten days of August. The model also suggests significant meltwater production in early September, in contrast to the three other years.

The last year of the series, 1995 (Fig. 4d), shows the smallest total, but highest single 10-d modelled meltwater production of all the years. Melting appears to start rather late in the ice area and never reaches the high amounts of calculated meltwater production from the firn area. In the last ten days of August, the model suggests that no additional ice area becomes exposed. This reduces total meltwater production to less than 1 m^3/s.

2.3 VERIFICATION OF MELTWATER PRODUCTION RESULTS

2.3.1 COMPARISON OF MODELLED AND MEASURED GLACIER MASS BALANCE

Table 3 shows the total specific net mass balance for the two absorption initialisations for snow, already mentioned in section 2.1.1. Whereas the value of 0.2 results in a rather good agreement for 1992 and 1995, it is poor for 1993 and 1994, even missing the sign of the net balance in 1993! This comparison led to the choice of the final absorption values for newly fallen snow. When one considers the uncertainties in the measured mass balance, which lie in the order of 250 mm w.e. (personal communication O. Reinwarth), the model performance can be considered rather good at this stage.

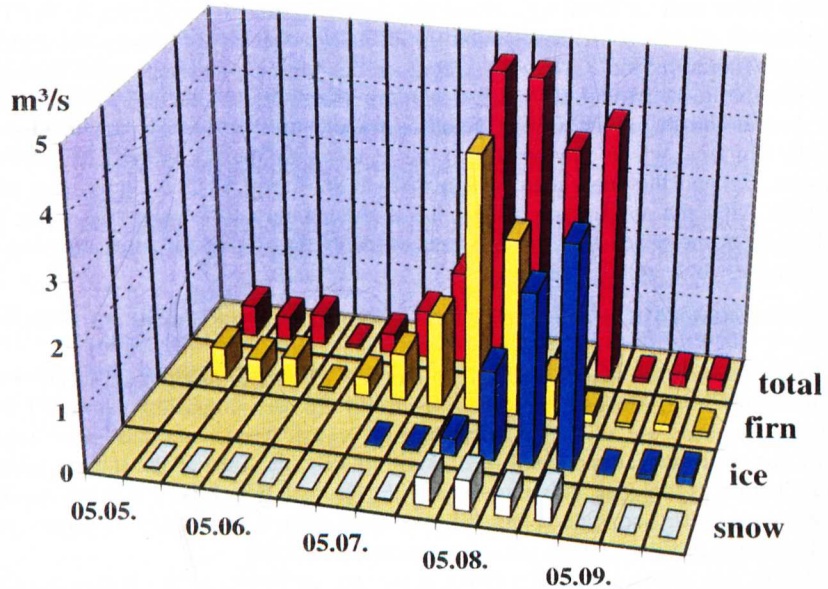

Fig. 4. Ten (eleven) day averages of meltwater production on Vernagtferner in $m^3 s^{-1}$, displayed separately for the three areal subunits snow (white), ice (blue), firn (yellow), and for the total glacier (red),
a) for the ablation period 1992

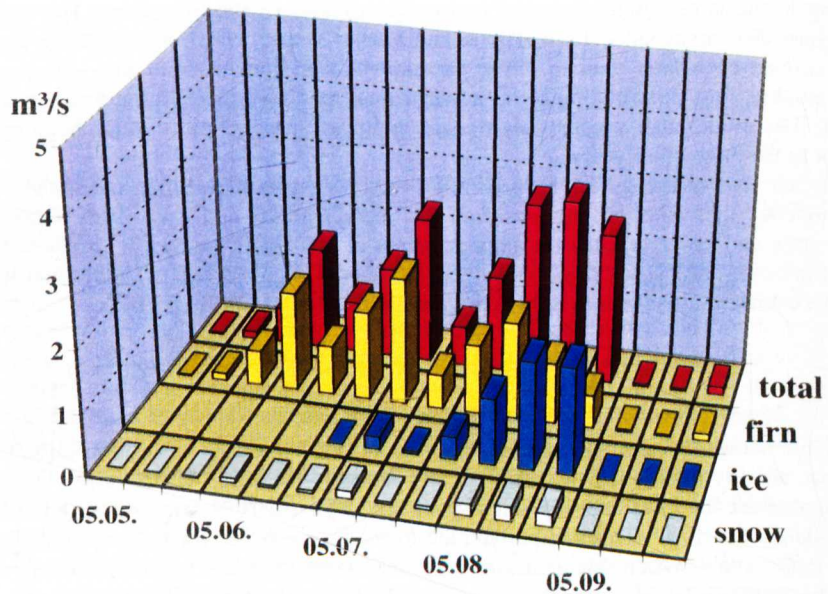

Fig. 4. b) for the ablation period 1993

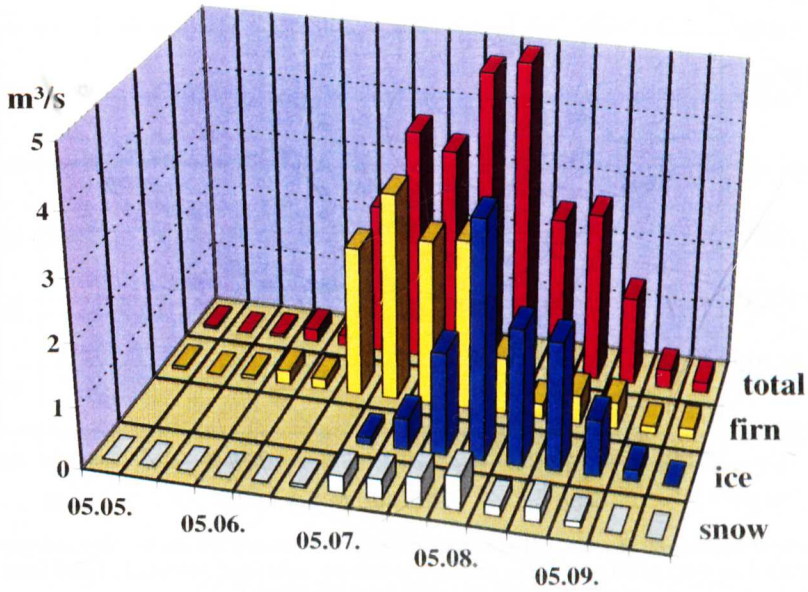

Fig. 4. c) for the ablation period 1994

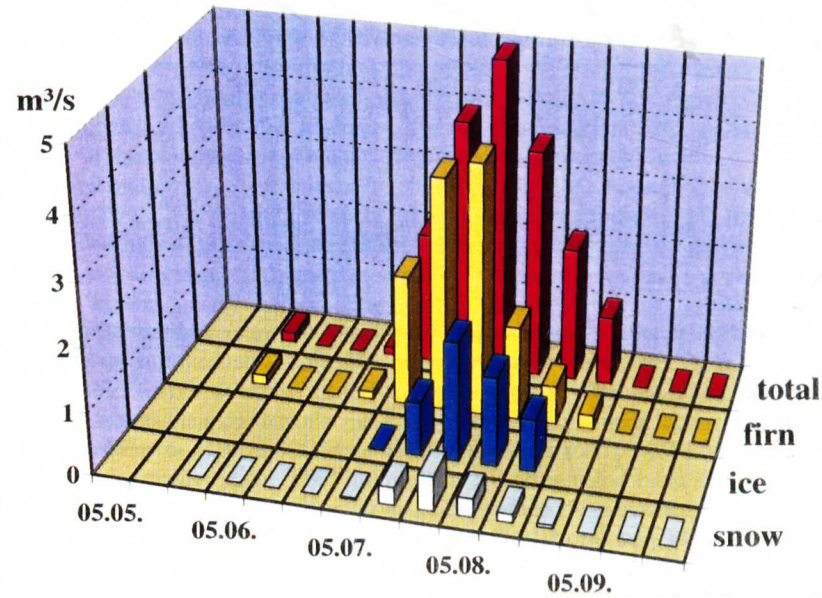

Fig. 4. d) for the ablation period 1995.

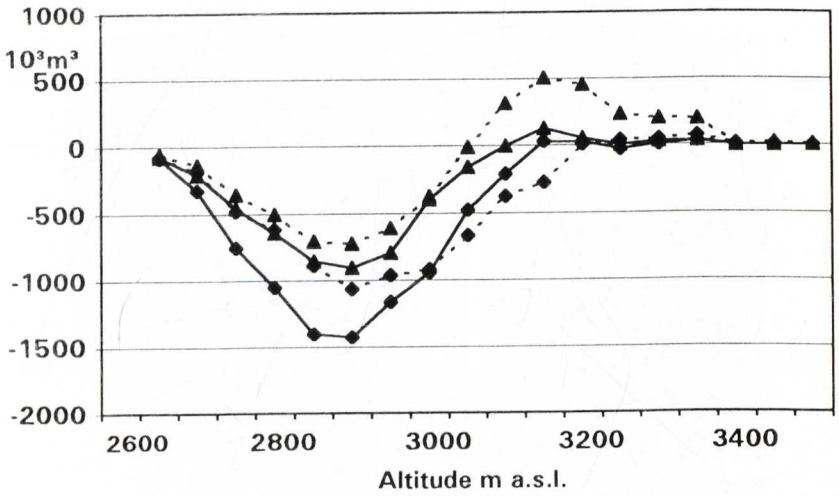

Fig. 5. Vertical distribution of measured and modelled net mass balance volume for Vernagtferner, in altitudinal intervals of 50 m, given in 1000 m^3; measured: solid lines; modelled: dotted lines; a) for the years 1992 (◆) and 1993 (▲)

Table 3: Comparison of modelled and measured total specific net mass balance b (mm w.e.) and equilibrium line altitude ELA (m a.s.l.) of Vernagtferner for the years 1992 to 1995 (case 1: absorption of newly fallen snow 0.2, case 2: absorption of newly fallen snow 0.3, measured: direct glaciological method)

	1992		1993		1994		1995	
	b mm	ELA m a.s.l.	b mm	ELA m a.s.l.	b mm	ELA m a.s.l.	b mm	ELA m a.s.l.
case 1	– 704	3300	368	3040	– 730	3325	– 207	3200
case 2	– 1125	3505	– 174	3200	– 926	3325	– 575	3280
Measured	– 858	3275	– 472	3250	– 1020	3300	– 398	3250

The modelled as well as the measured profiles of the vertical distribution of mass balance for 1992 (Fig. 5 a) clearly demonstrate the difficulty of determining a reasonable ELA, as both model and measurement show very small mass balances above 3300 m a.s.l.. Compared with the model distribution, measured values show higher mass losses in the range below 3100 m and lower ones between 3100 m and 3300 m, but, as a whole, the balance profile is matched not too badly by the model. For 1993, model values are generally more positive than measured ones, and agreement is better in the ablation area than in the accumulation area. The profiles of 1994 (Fig. 5 b) depict the highest mass losses of these four years, with no noticeable accumulation left in the entire altitudinal range, revealed both by model and measurement. Modelled and measured mass balance data agree best in the ablation zone for the year 1995.

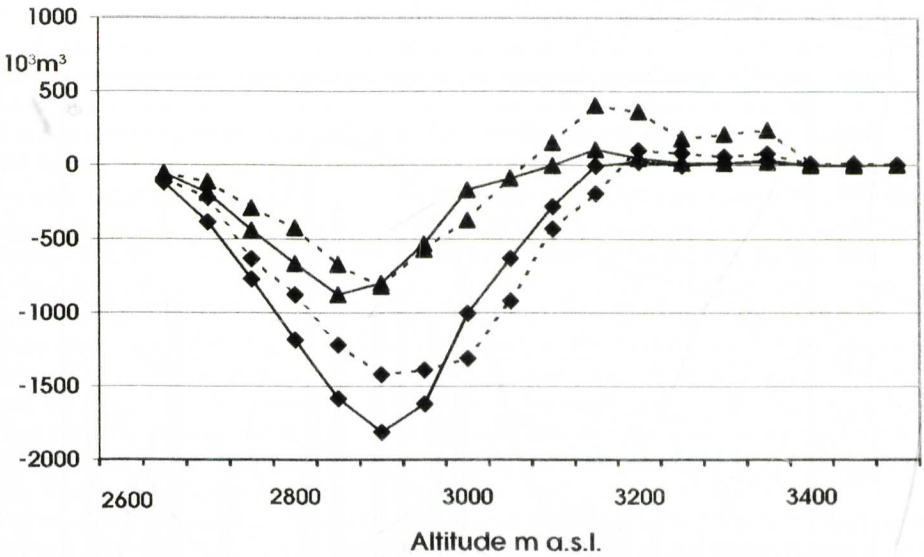

Fig. 5. b) for the years 1994 (◆) and 1995 (▲).

2.3.2 COMPARISON OF THE EVOLUTION OF MODELLED AND PHOTOGRAPHICALLY DERIVED ICE AREA SIZE

The growing and diminishing of ice area during the ablation period is also validated with photographic data. Since 1978, 60 % of the glacier area of Vernagtferner is photographed once a day during the ablation season with an automatic camera (c.f. Fig. 1 for the sector of photographic survey). From these photographs, the size of the bare ice area for selected days can be evaluated by mapping all pixels which lie in this region. The ice area, however, is underestimated by this procedure due to the incomplete coverage and small spatial resolution of the photographs in the flat middle region of Vernagtferner.

With these irritations in mind, Figure 6a shows that in 1992 the modelled ice area starts to increase somewhat more slowly than the photographic data indicate, but during August, model values are higher than measured ones. Modelled snowfall at the beginning of September on the whole glacier surface is in agreement with observation. The melting of this summer snow in the second half of September is also depicted by the model, although agreement with observation is poor. Considering all the approximations and assumptions in the modelled ice area growth, however, the agreement is acceptable.

For 1994 (Fig. 6b), model and observation agree better. The onset, development, decrease, and eventual disappearance of the ice area from the beginning of July to the middle of September is modelled rather well. On 24 August, a photo survey of the complete glacier surface was made. Thus, for this day, measured and modelled values should agree fairly well – which they do. Based on the 24 August photographs, the maximum ice area extent was estimated for the rest of the summer, so photo analysis and model values should show the same results. However, the model appears to underestimate the ice area size after the snowfall on 3 September, most probably due to poor timing of the precipitation event.

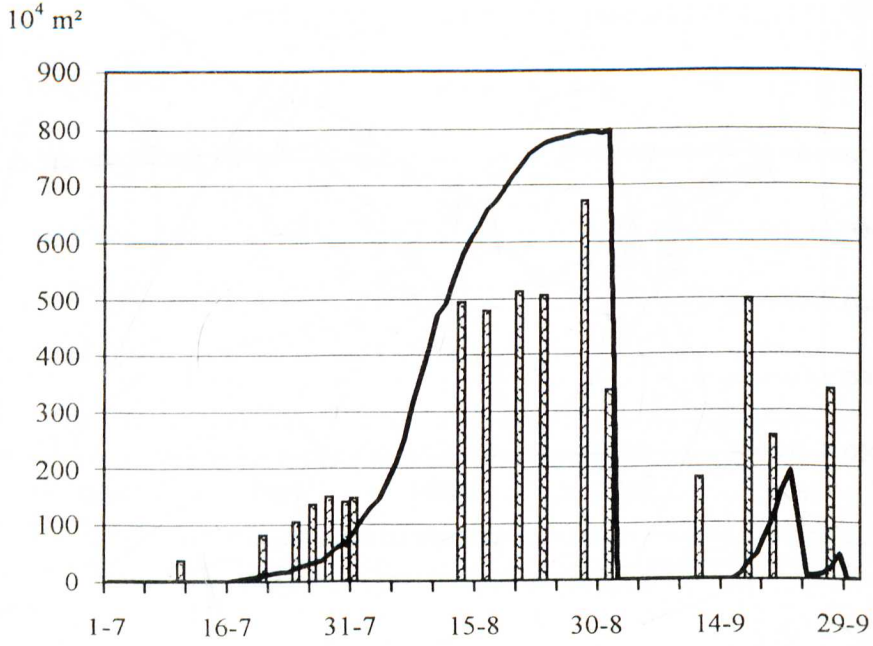

Fig. 6. Comparison of the recorded and modelled temporal development of the size of the bare ice area on Vernagtferner in ha (10^4 m^2). Columns represent the results of the photo analyses, continuous lines show the modelled values. The total glacier area is 9.1 km^2.
a) July to September 1992

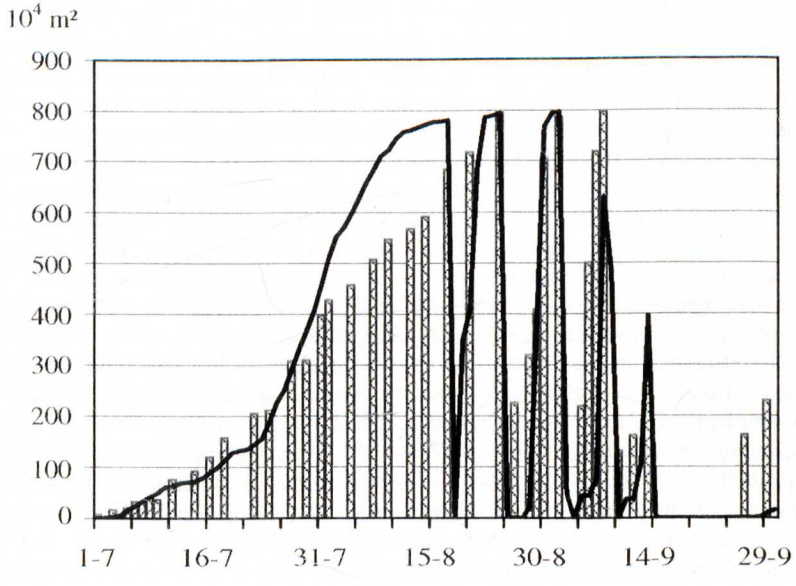

b) July to September 1994.

2.3.3 MODELLED SPATIAL DISTRIBUTION OF ABLATION, ALBEDO AND ICE AREA

As the modelled spatial and temporal development of the ice area is a result of the complete energy balance determination of the glacier surface, Figs. 6a and 6b give us more confidence in the model results than the comparisons with mass balance data. However, it is also relevant to determine whether ice appears at the right place on the glacier surface. This will be demonstrated by using four examples from the year 1993.

Compared to 1992, 1994, and 1995 (Table 4), 1993 is characterised by high precipitation sums of July plus August, low air temperature averages in July. This leads to repeated snowfall events, especially in the higher regions of Vernagtferner. The model results reflect this weather pattern rather well. Figure 7a is from 10 July. Blue colours in panel I indicate that a considerable amount of winter snow still covers the glacer, whereas green areas signal the onset of ice ablation. Therefore, the modelled (82 ha) and actual ice areas (80 ha) (blue in panel III, dark in IV) are rather small. In the lower part of the glacier (c.f. Fig. 1 for the altitudinal distribution of Vernagtferner), the distribution of modelled bare ice patches matches the observed one. This does not hold for the upper part of the glacier, where several bare ice spots (panel IV) are not calculated by the model (panel III). This is probably because of the low spatial resolution of the initial snow cover data. The modelled firn albedo (panel II) increases with altitude because little or no melting has reduced the fresh snow in the upper regions. Beige spots in all the panels represent areas free of ice.

Table 4: Monthly sums of precipitation P [mm] and averages of air temperature T [°C] for the ablation seasons 1992 to 1995 at the Pegelstation Vernagtbach

	1992		1993		1994		1995	
	P	T	P	T	P	T	P	T
May	21	1.7	58	1.9	84	1.0	64	−0.1
June	107	3.4	93	4.5	74	4.0	99	1.7
July	95	7.4	156	5.1	102	8.2	100	8.3
August	69	9.0	107	6.9	117	7.8	107	4.8
September	53	4.3	81	2.3	125	3.8	70	1.0
Sum/average	345	5.2	495	4.1	502	5.0	440	3.1

Figure 7b shows the conditions for 30 July 1993. Ice area has increased in the model (panel III) as well as in reality (panel IV) (159 ha and 157 ha, respectively), with rather similar areal distributions. Low melting on north facing slopes (c.f. Fig. 1) along the southern glacier margin is perceived rather well by the model, as is the patchy development of ablation in the middle part of the glacier (panel I). Snowfalls from 11 to 14 and 20 to 22 July over the entire glacier region have increased net mass balance to 1200 mm w.e. in regions above 3400 m a.s.l. (c.f. Fig. 1), whereas ice ablation was only interrupted by these spells of bad weather, but continued on the remaining days. This is indicated by green to yellow colours in Panel I, signifying that ablation has reached values of more than − 700 mm w.e. in the 2750 to 2800 m interval. Another consequence of these snowfalls is that the areal pattern of albedo for 30 July (panel II) does not deviate significantly from that of 10 July.

In the period between 30 July and 12 August, snowfalls on 31 July and from 9 to 11 August have affected only the upper regions of Vernagtferner. Thus, after the ice area has increased to 339 ha (modelled) or 250 ha (measured) by 7 August, it is reduced to

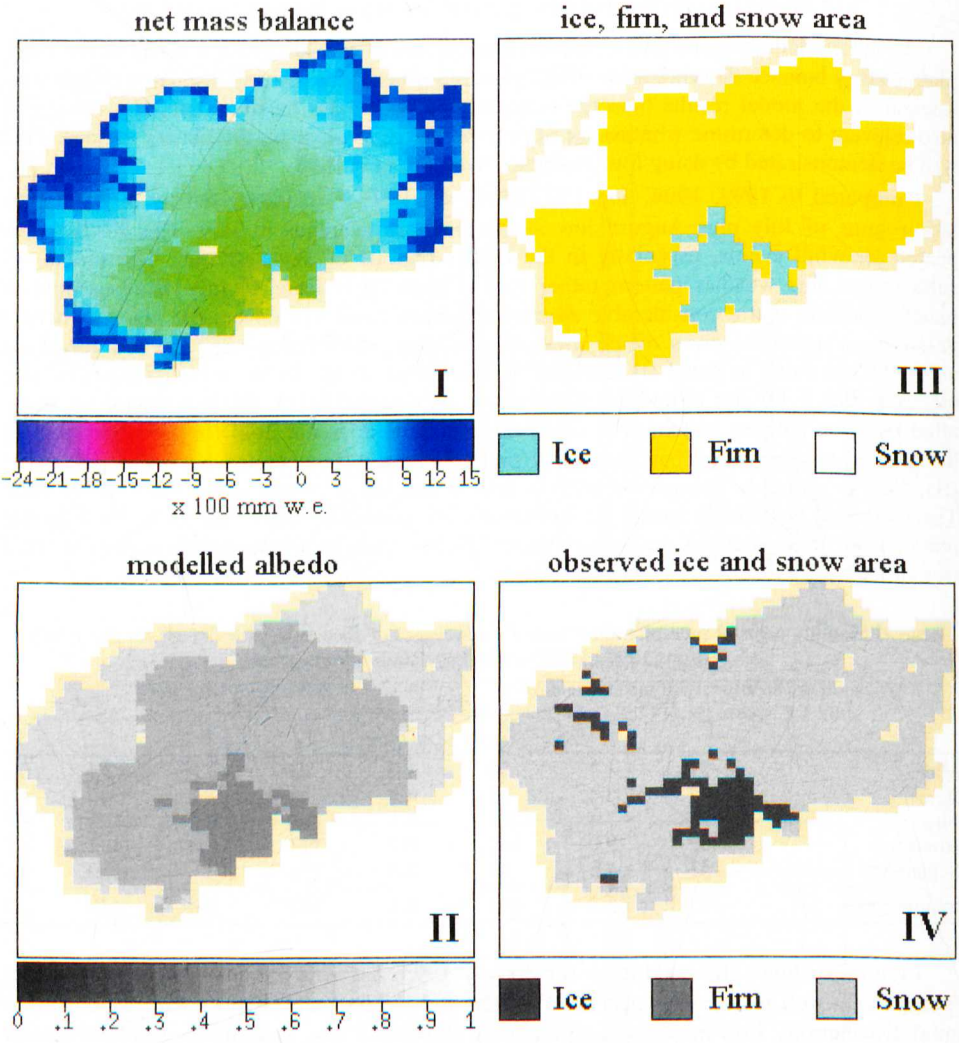

Fig. 7. Temporal and spatial development of:

I) net mass balance (100 mm w.e.)
II) modelled albedo
III) modelled distribution of ice, firn and snow area
IV) recorded distribution of ice and firn or snow, respectively
for the following days
a) 10 July, 1993

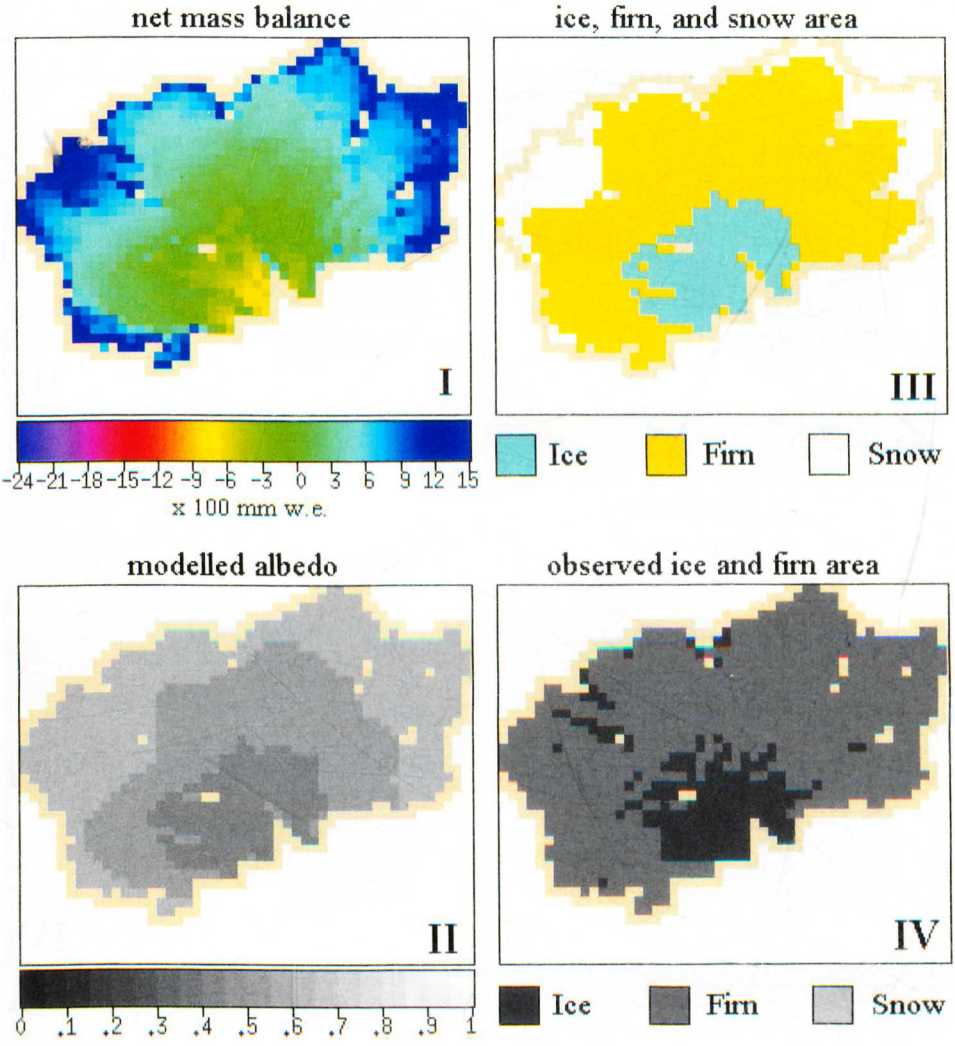

b) 30 July, 1993

values of 156 ha (modelled) or 148 ha (measured) on 12 August (Fig. 7c), displaying a good agreement in their respective areal patterns. Therefore, ice melt continues over the whole time at altitudes below 3000 m a.s.l, illustrated by yellow to red colours of net mass balance (panel I), whereas accumulation prevails in the uppermost part of Vernagtferner.

Figure 7d for 26 August 1993 demonstrates the conditions before the end of the "natural" ablation season. The difference of modelled and measured ice area for 26 August (panels III and IV, respectively) has to be attributed to the photographs. Total modelled ablation was -1800 mm w.e. or $-500 * 10^3$ m^3 w.e. in regions below 2900 m a.s.l. (c.f. Fig. 1), while positive mass balances of up to 1400 mm w.e. above 3400 m a.s.l. indicate an

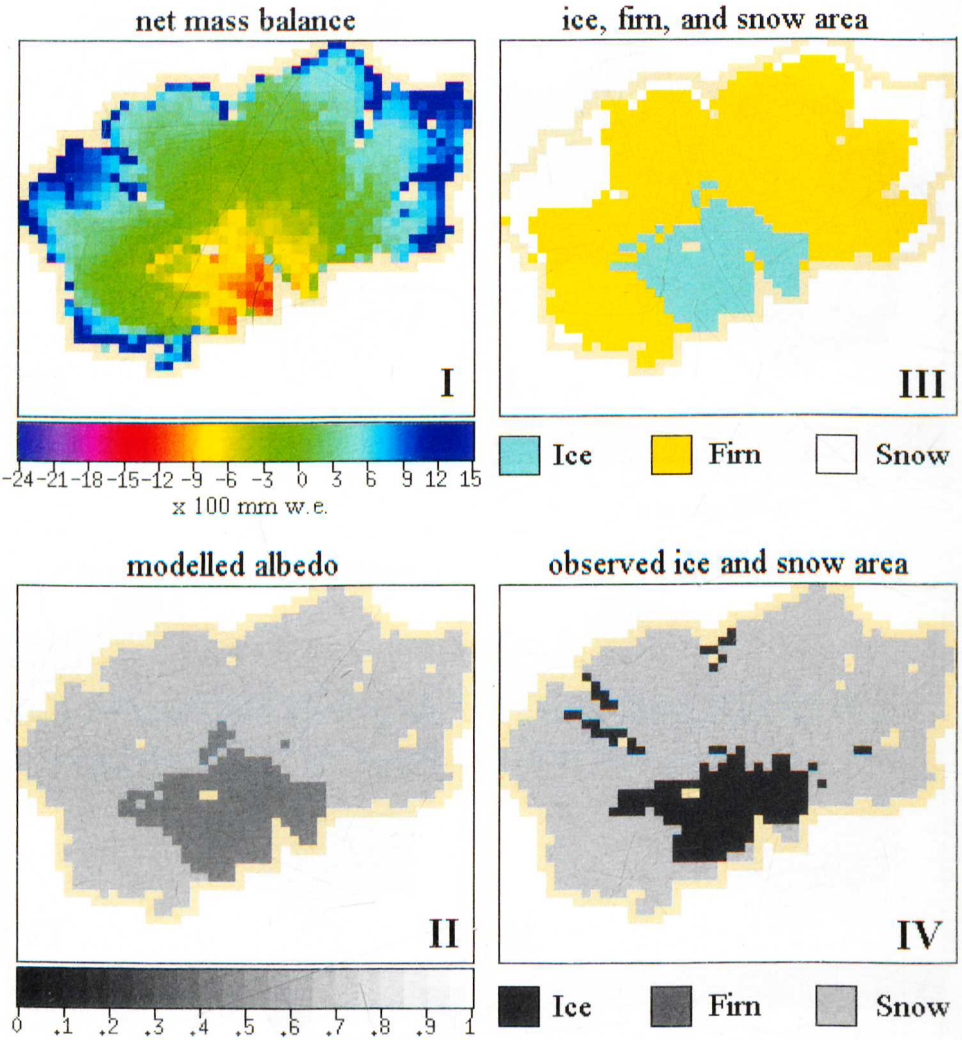

c) 12 August, 1993

additional modelled accumulation during the summer (c.f. Fig. 3 for comparison to winter snow cover and Fig. 5a for the altitudinal mass balance volume distribution on 30 September 1993).

As a whole, the meltwater production model can be assumed to reflect real processes to a high degree. Starting from the winter snow cover, the evolution of the ice area is a sensitive indicator of the performance of the model, as it results from all the assumptions of the melting routine. The good agreement with observation in the temporal and spatial pattern allows us to have some confidence in the albeit sometimes rather simple model structure. In

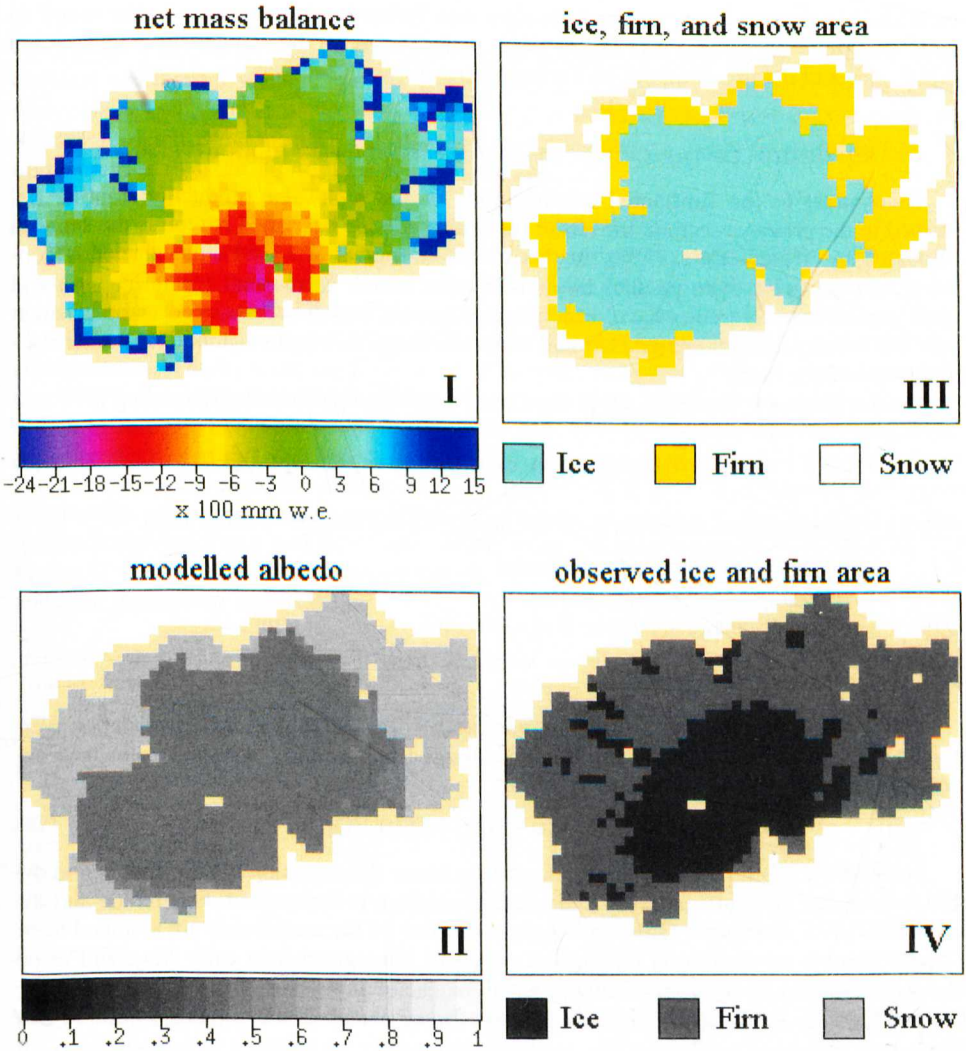

d) 26. August, 1993

the next part of the paper, this is confirmed by a total difference between modelled and recorded discharge over the ablation season of 7 % in 1992, 9 % in 1993, and 5 % in 1995.

3. RUNOFF FROM VERNAGTFERNER

The runoff pattern in the 1990's is quite different from that of the early 1980's, when Vernagtferner was in a nearly balanced state. Since the end of the last decade, ever increasing mass losses have led to a continuous shrinkage of the firn cover of the glacier, already

mentioned in section 2.2.1. As these changes may influence the formation of the runoff to quite an extent, the second part of this paper concentrates on the changes in boundary and initial values of the runoff model, as the model architecture itself was not altered.

3.1 DESIGN OF THE LINEAR RESERVOIR MODEL FOR VERNAGTFERNER

In contrast to the substantial modifications of the meltwater production routine described in the previous section, the runoff modelling routine described hereon is the same as discussed by Moser et al. (1986). In this model (Oerter et al., 1981), the glacier is considered to comprise three parallel linear reservoirs, which correspond to the ice, firn and snow area. These reservoirs have recession coefficients, which are assumed to be constant over the whole ablation season. Ground water discharge is constant, too. The model uses time steps of one hour.

On this basis, the discharge, $Q_i(t)$, from each reservoir, i, is modelled according to

$$Q_i(t) = \int_0^t ((S_i(\tau)/k_i)(\exp((\tau - t)/k_i)))d\tau + Q_i(0)\exp(-t/k_i) \quad (7)$$

where i is the number of reservoir, (i = 1 ice area, i = 2 firn area, i = 3 snow area).

S_i	meltwater production in reservoir i	$m^3\ s^{-1}$
k_i	recession coefficient of reservoir i	s
$Q_i(0)$	initial discharge at time t = 0 of reservoir i	$m^3\ s^{-1}$
t	time	s
τ	variable of integration.	s

The total model discharge $Q_m(t)$, representative for the site of the Pegelstation Vernagtbach, is determined by the sum of the discharge from the three reservoirs plus the constant groundwater component $Q_4 = 0.1\ m^3\ s^{-1}$

$$Q_m(t) = Q_1(t) + Q_2(t) + Q_3(t) + Q_4. \quad (8)$$

To solve eq. (7) for each reservoir, one has to know the recession coefficients k_i and the initial discharge amounts, once the meltwater production is determined. For the ice and the snow reservoirs, discharges $Q_1(0)$ and $Q_3(0)$ at the start of the model runs are assumed to be zero, as there is no melting in the highest region of Vernagtferner in early May, and as no water is in the ice reservoir at midnight, when the calculations start. Thus, $Q_m(0) = Q_2(0) - Q_4$, and $Q_2(0)$ is set to $Q_r(0)$, which is the recorded discharge at the gauging station at that time.

The most crucial parameter in this discharge modelling approach is certainly the recession coefficient of the individual reservoir. In various field and numerical studies in the course of the SFB 81 research program, a broad range of values for these parameters was found (Oerter et al., 1981). Without going into detail, the results of these analyses will be summarised, as they are discussed in the present study as well. For the ice reservoir, values for k_1 of 4 to 9 hours were determined; k_2 turned out to be 20 to 60 hours, and k_3 140 to 620 hours. As was observed as well as expected in these early investigations, the values were not constant over the course of the ablation season, owing to the development of the internal hydrological system of the glacier. Nevertheless, for the model runs of 1978 to 1985 (Escher-Vetter et al., 1986; Moser et al., 1986), 4 h, 30 h and 430 h were used as typical averages for the whole ablation season.

3.2 DISCHARGE MODEL RESULTS

All the comparisons of modelled and recorded runoff are based on the assumption that the total runoff from Vernagtferner is running through the gauge, that is there are no subsidiary streams which by-pass the station. Extensive experimental studies in the course of the SFB 81 research program have substantiated this assumption – with the exception of extreme cases such as mentioned in the next paragraph!

3.2.1 STATISTICAL MODEL EVALUATION

Table 5 gives the result of the statistical quality control of modelling hourly discharge. Here, the efficiency criterion R^2 (Nash and Sutcliffe, 1970) is presented for various combinations of recession coefficients of bare ice area (k_1) and firn area (k_2). The recession coefficient of snow area, k_3, was set constant at 430 h. For the years 1992, 1993 and 1995, five combinations of k_1/k_2 were used, i.e. 4/80, 4/40, 8/40, 6/80 (for 1992 and 1993) and 6/40 (for 1995). For 1994, it is not possible to determine R^2, as discharge recordings were disturbed in July and completely interrupted at the beginning of August. Extremely high meltwater production in this year led to discharges of more than 15 $m^3 s^{-1}$, damaging the gauge, and surpassing the maximum design discharge by more than 50 %. This was the first severe interruption after a 20 years time series of discharge recording at the Pegelstation Vernagtbach (Escher-Vetter and Reinwarth, 1994). Peak discharge conditions are illustrated in Figure 8, with water not only running through the measurement channel, but also around it and even through the station cabin.

Table 5: Nash-Sutcliffe efficiency criterion R^2 for various combinations of recession coefficients for the bare ice reservoir k_1 (hours) and the firn reservoir k_2 (hours), determined for the whole ablation seasons (V–IX) and the period July/August (VII–VIII) of the years 1992, 1993, and 1995

k_1/k_2	1992		1993		1995	
	V–IX	VII–VIII	V–IX	VII–VIII	V–IX	VII–VIII
4/80	0.637	0.473	0.851	0.787	0.711	0.329
4/40	0.678	0.557	0.836	0.792	0.753	0.430
8/40	**0.793**	**0.792**	0.851	0.821	**0.837**	**0.638**
6/80	0.746	0.693	**0.876**	**0.833**	–	–
6/40	–	–	–	–	0.822	0.601

For the three remaining years, two periods each were analysed; the entire ablation season (V–IX) and the two months with major runoff, July and August (VII–VIII). Although the combinations of k values are in the range of those applied in the 1980's, the differences indicated by differing model efficiency are obvious. The first is, that higher values of k_1 give a better performance than lower values in 1992 and 1995, whereas in 1993, the coefficients do not deviate significantly from each other for all k-combinations. The second is that, in 1993 and especially in 1995, R^2-values for July/August of all years and all k-combinations are lower than those of May to September. This could be caused by the fact that the recession coefficients are not constant over the summer.

3.2.2 DISCHARGE MAXIMA AND MINIMA: COMPARISON OF MODELLED AND RECORDED AMOUNTS

Let us now compare the modelled and measured amounts of daily discharge maxima and minima during the ablation season for those $k_{1,2}$-combinations, which yielded the best results in Table 5. Figure 9a displays the results for the discharge maxima in 1992. The re-

Fig. 8. On 3 August 1994, peak runoff occurred at the Pegelstation Vernagtbach, damaging the recording device (Photo by G. Patzelt).

lationship is not far from linear, with a correlation coefficient of 0.90. For measured maxima between 2 $m^3 s^{-1}$ and 4.5 $m^3 s^{-1}$, the model underestimates the records, whereas maxima of more than 5 $m^3 s^{-1}$ are sometimes overestimated by model values. This may be caused either by too high meltwater production or by too fast emptying of the ice reservoir. Considering the meltwater production modelling results, however, it is more likely that the differences are caused by discharge modelling.

Figure 9b depicts the same quantities for 1995. Here, the agreement is somehow better, confirmed by the higher correlation coefficient of 0.92. As in 1992, however, most of the modelled maxima in excess of 4 $m^3 s^{-1}$ are higher than the measured ones. This is reflected in the smaller Nash-Sutcliffe efficiency criterion of 0.638 in Table 5 for July/August, the only period when these high maxima are observed.

The relation between modelled and measured minima (Fig. 10) is also nearly linear,

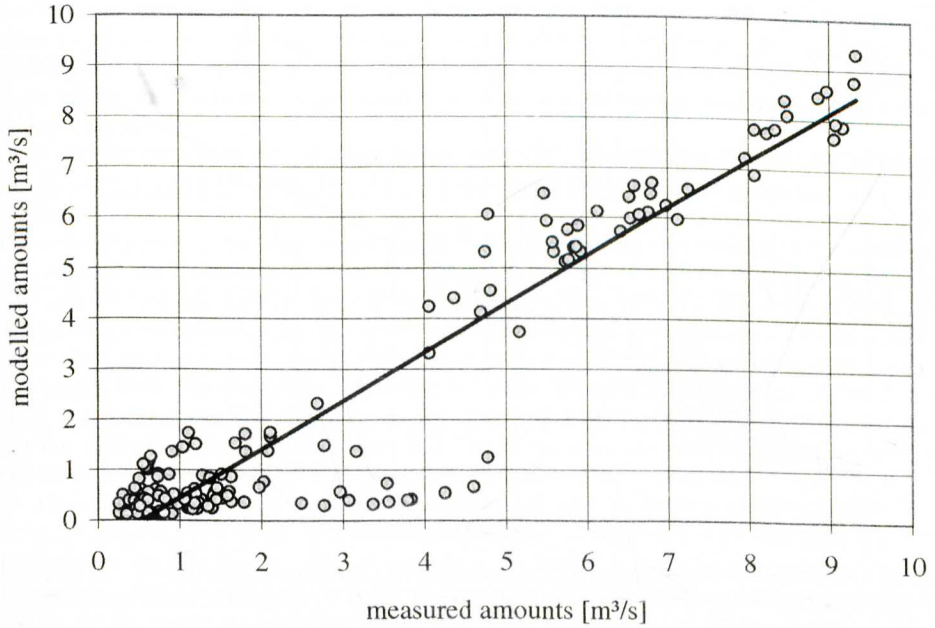

Fig. 9. Linear correlation of modelled (Q_m) and recorded (Q_r) discharge maxima in $m^3\ s^{-1}$ at the Pegel-station Vernagtbach for the ablation seasons of
a) 1992 ($Q_m = -0.53 + 0.96\ Q_r$, corr. coefficient = 0.90)

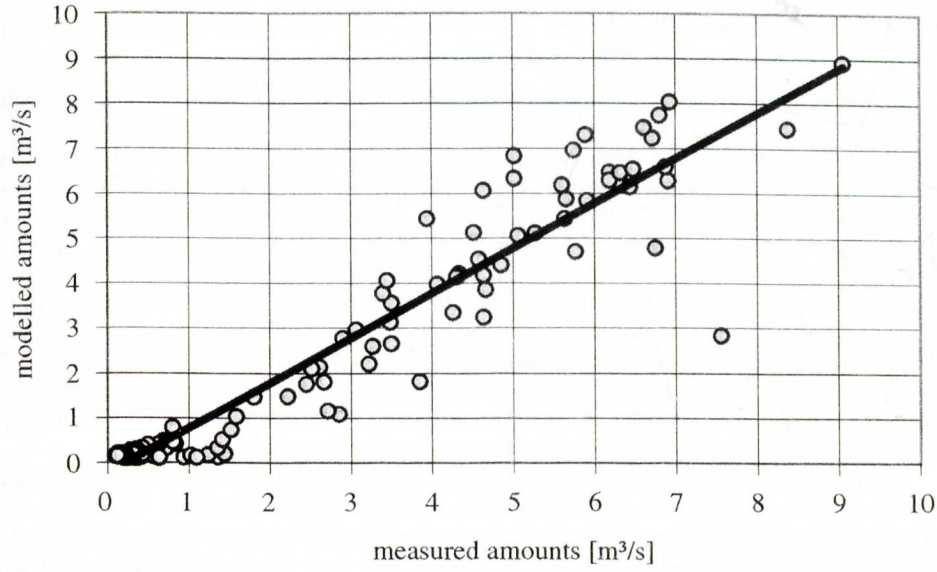

Fig. 9. b) 1995 ($Q_m = -0.23 + 0.99\ Q_r$, corr. coefficient = 0.92).

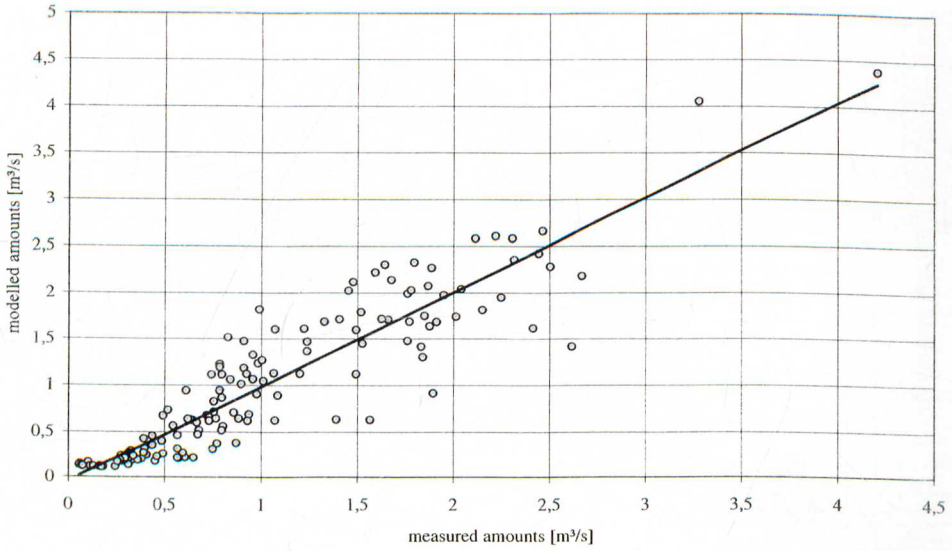

Fig. 10. Linear correlation of modelled (Q_m) and recorded (Q_r) discharge minima in $m^3\ s^{-1}$ at the Pegelstation Vernagtbach for the ablation season 1993 ($Q_m = -0.04 + 1.02\ Q_r$, corr. coefficient = 0.85).

with the smallest offset but also the smallest correlation coefficient. Noticeable is the maximum value of 4.2 $m^3\ s^{-1}$ which was recorded as well as modelled for 23 August 1993, the day with the highest discharge average of the year, e.g. 6.0 $m^3\ s^{-1}$.

3.2.3 TIME SERIES OF MODELLED AND MEASURED DISCHARGE

Figure 11 gives model results for the entire 1992 ablation period. During May, June, and part of July, the modelled values are sometimes higher and sometimes lower than recorded discharge data, resulting in a difference not larger than ~ 1 $m^3\ s^{-1}$ for individual hours. The diurnal variation of discharge in spring is dominated by the recession coefficient for the firn area. Although the value of 40 h was derived for firn and snow depths up to 20 m originally, it fits rather well for the 1–4 meters of winter snow which cover the glacier in May. In June, however, a value of 20 to 30 h for k_2 would result in a better agreement between modelled and recorded discharges. From 20 July to the end of August, the deviations increase up to 3 $m^3\ s^{-1}$, yielding model results which are systematically too high. This is most likely associated with the modelled runof from the bare ice section. A recession coefficient k_1 of 9 to 10 hours would give a better agreement during this period. The underestimate of the recorded discharge in September, however, is caused by erroneous meltwater production modelling, as the energy balance model predicted a bare ice area smaller than observed.

The design of Figure 11 gives a good overview of the model performance for the entire ablation period, but makes it difficult to further study individual features. Therefore, the modelled and recorded time series of discharge for July and August 1993 and 1995 are presented in Figs. 12a and 12b. As could be expected from the high R^2 value of 0.833 (Table 5) and the rather good correlation coefficients for the minimum amounts (Fig. 10),

the discharge variations in 1993 are represented rather well by the model, with smaller differences only on the days when bare ice reappears after a snowfall (e.g. 15 to 20 July). The diurnal cycle in the difference curve from 28 July to 25 August is most likely caused by a slight phase shift between model and records, as the absolute maximum and minimum amounts agree well.

For 1995, the results for July and August give a slightly different picture (Fig. 12b). As was also observed in 1993, the bare ice area developed rather late, and as a result, discharge in July is dominated by the output from the second reservoir. This leads to small amplitudes, mainly caused by high minima, during the first twenty days. Calculation, however, uses a recession coefficient of 40 h – compared to the 80 h for 1993. For the last third of July and the first ten days of August, the model depicts smaller diurnal amplitudes of discharge as it overestimates the minima, and sometimes also the maximum amounts. For a rather short time span in the middle of August, only, modelled and recorded discharge agree reasonably well. An exception is 15 August, when modelled ice discharge is much too small (c.f. largest negative deviation in Fig. 9b). Here, the energy balance model predicts that the altitude of the temporal snow fall line is too low, resulting in a bare ice area of 213 ha which is much smaller than the 460 ha derived from the photograph.

The influence of the precipitation modelling can also be demonstrated with data from 22 to 24 August 1993 (Figs. 12a and 13). 22 August was the day with the highest hourly discharge of the first twenty years of recording, 10.7 $m^3 s^{-1}$, caused entirely by melting. In the evening, a thunderstorm occurred with 5 mm precipitation, falling as rain over the entire glacier. As the model precipitation for the whole day is attributed to the first hour (c.f. 2.1.2, precipitation), the thunderstorm contribution is modelled too early, leading to an underestimation of 2.6 $m^3 s^{-1}$ modelled discharge in the evening. On 23 August, rainfall started already in the morning and lasted during the whole day, summing up to 25 mm. For this day, the modelled diurnal variation of total discharge agrees better with the recorded one.

Figure 13 also provides a detailed view of the interaction of the various reservoirs, displaying the discharge components for August 1993. At the beginning of the month, the discharge from the bare ice area, Q_1, contributes less than half of the total, whereas in the second half of August, discharge from the firn reservoir, Q_2, has decreased considerably, due to the shrinking of the corresponding reservoir area. Discharge from the highest region of Vernagtferner, Q_3, is very small, with nearly no variation throughout the month, caused by the low meltwater production sums in this region (c.f. Fig. 4b). The precipitation event on 23 August is reflected in the ice and firn reservoir discharge, as the typically rapid decrease of the ice reservoir output during the early morning hours is interrupted by the additional rainfall input, resulting even in a slight rise in modelled discharge values of Q_1. The rainfall in the firn area prevents the typical decline of the discharge, and, as a result, the green curve remains nearly constant during this day and the next. Decreasing air temperatures lead to snowfall above 3490 m a.s.l. on 24 August and above 3190 m a.s.l. on 25 August (daily means). This is rather well reflected in the model not only by the decrease of the firn reservoir output, but also by the smaller amounts of the ice discharge, Q_1, on 25 August.

4. SUMMARY AND CONCLUSIONS

It was the purpose of this paper to present the results of a study of meltwater production and runoff modelling for Vernagtferner, one of the larger glaciers in the Oetztal Alps. This modelling is based on extensive research, started in the late 1970's within the framework of

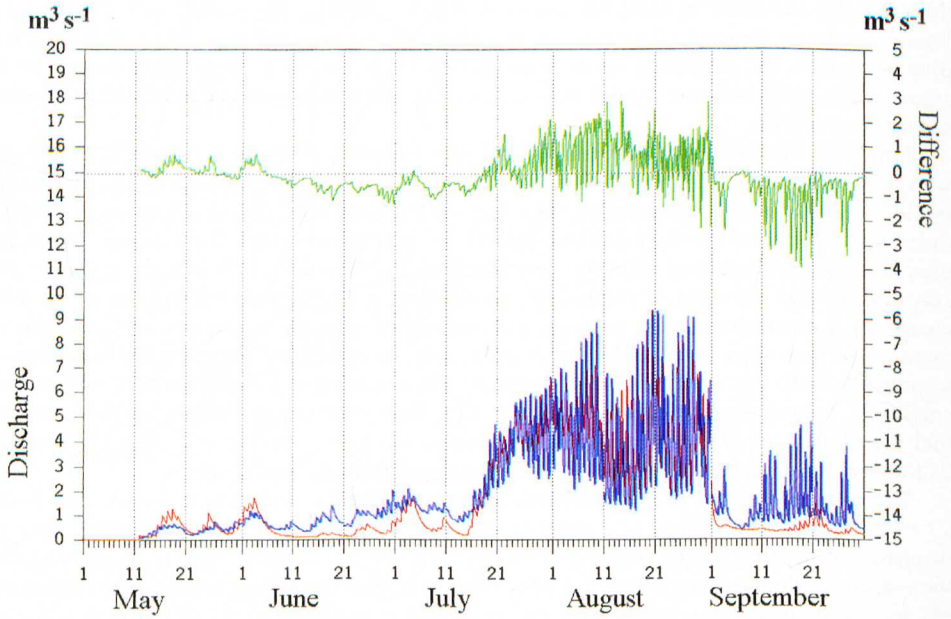

Fig. 11. Hourly values of recorded discharge Q_r (blue), modelled discharge Q_m (red), and the absolute difference ΔQ (green, positive values: model overrates record) for the 1992 ablation period. Model results obtained with $k_1 = 8$ h, $k_2 = 40$ h, $k_3 = 430$ h.

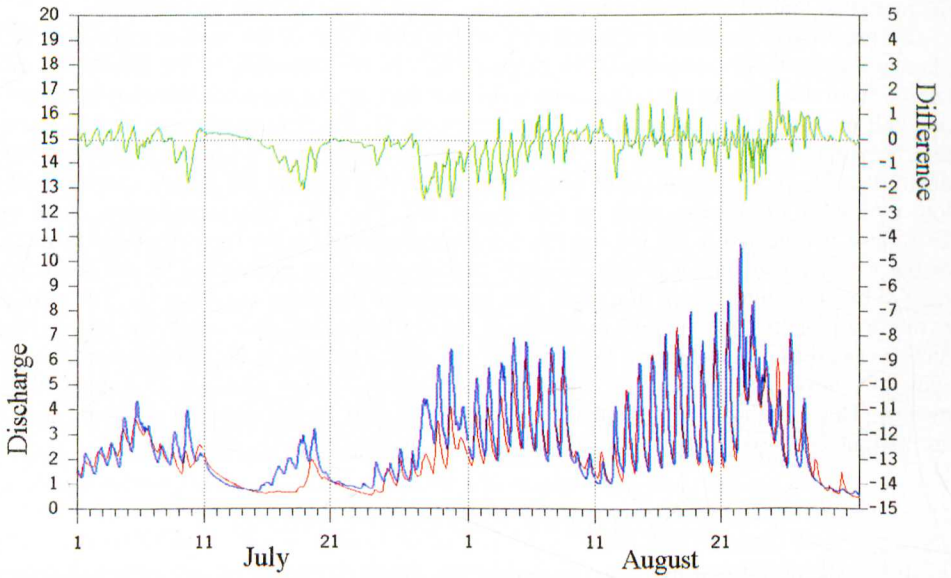

Fig. 12. Hourly values of Q_r (blue), Q_m (red), and ΔQ (green) for:
a) July and August 1993; model results obtained with $k_1 = 6$ h, $k_2 = 80$ h, $k_3 = 430$ h,

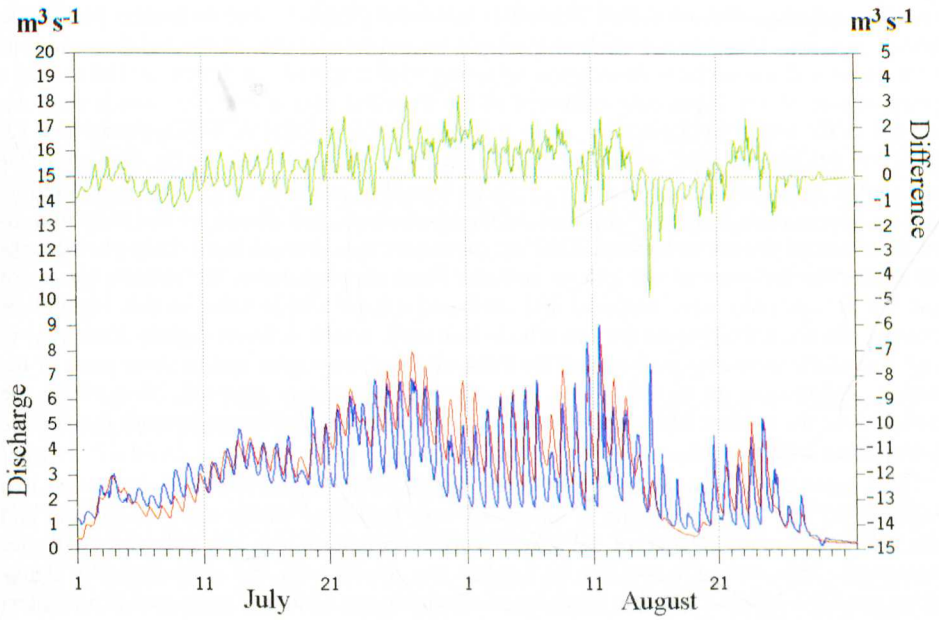

Fig. 12. b) July and August 1995; model results obtained with $k_1 = 8$ h, $k_2 = 40$ h, $k_3 = 430$ h.

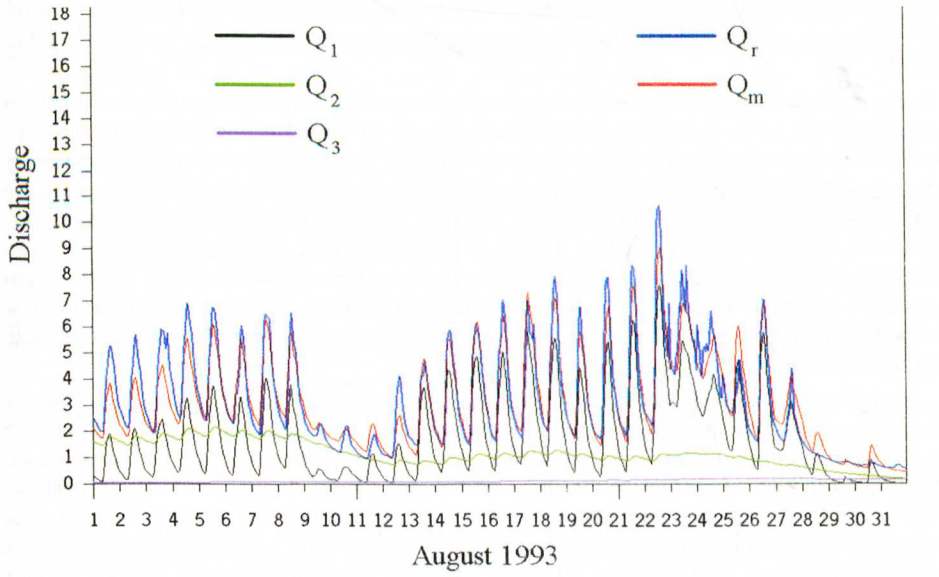

Fig. 13. Hourly values of total discharge and its modelled components for August 1993, using the same k_1/k_2 values as in Figure 12a: ice reservoir component Q_1 (black), firn reservoir component Q_2 (green), snow reservoir component Q_3 (magenta), Q_m (red), Q_r (blue) (c.f. Equation (8)).

a special research program called "Runoff in and from glaciers". The meltwater production model, then developed, was based on a simple formulation of the energy balance equation for a snow and ice surface, calculating all terms with a spatial resolution of 100 m and a temporal one of 1 h. Input data consisted of (1) recorded data at one site, which were expanded to the entire catchment by using a Digital Terrain Model of Vernagtferner and (2) indirectly determined data, which were partly based on recorded ones. In the first group we find global radiation, air temperature, relative humidity, wind velocity, and precipitation. Surface temperature, longwave radiation of the atmosphere, and albedo are the most important members of the second group. This last parameter was derived from daily photographs which display the state of the glacier surface. From these pictures, the relative shares of bare ice for each day were analysed and attributed a fixed albedo value of 0.4. For the remaining glacier, a fixed value for firn albedo was used, which differed slightly from year to year. Snowfalls were also analysed on the basis of the photographs, and in those parts of the glacier, albedo was set to 0.8. Thus, the only two parameters internally derived by the model, were the surface temperature and the cold content of the layers beneath the surface during times without melt.

This basic model has been further developed to some extent. Most important are two changes: (1) The melting routine is initialised with measured winter snow cover data and thus, the actual mass balance of the glacier surface is determined, not only the meltwater production. This makes it possible to validate the results with the glaciologically determined net mass balance. (2) The decrease of albedo due to ageing of snow and firn is internally derived by the model, and the ice area size results from the melting of this snow cover. Therefore, the photographs can now be also used for validation. Precipitation type is also modelled on the basis of the altitudinal temperature distribution, so snowfall amounts and distribution also become internal parameters. Thus, the absolute values of the absorption coefficients of the different materials are the only data which have to be supplied additionally.

The modular design of the former approach was not altered, so, further improvements in single parts can be incorporated without the necessity of a total change of model architecture. This is most important for the parameterisation of the heat fluxes, which, as repeatedly mentioned, uses an extremely simple approach, which can be substantially improved by the results of the investigations of the HyMEX program. HyMEX is a research program on Vernagtferner, which was performed in August 1998 and led to a re-evaluation of lapse rates and wind velocity distributions, which will be discussed in a separate paper. Another improvement could be achieved by a higher temporal resolution of the precipitation records. Nevertheless, meltwater production, as it is determined with this simple physical model, can be assumed to reflect real processes to a high degree.

In the second part of the paper, the runoff is investigated, using modelled meltwater amounts as input. For the four years under investigation, recorded and modelled discharge amounts for the entire ablation season differ only by 5 % (best case) to 9 % (worst case). As the hydrological conditions of the early 1990's have changed quite markedly from those of the early 1980's, a statistical analysis of the recession coefficients, previously used, was performed for the different regions of Vernagtferner. Based on the coefficients with the best correlation numbers, the time series of recorded runoff is reproduced quite well by using a linear concept with three reservoirs, applying constant values for the recession coefficients of the ice area, k_1 (8 h and 6 h, respectively), of the firn area, k_2 (40 h and 80 h, respectively), and of the uppermost region of the glacier, k_3 (430 h). The agreement, however,

could be improved to some extent, when the values are adapted to the changes in the hydraulic conditions within the glacier in the course of the ablation season.

ACKNOWLEDGEMENTS

The author is indebted to all the co-workers, who helped in the field and evaluation work; especially Markus "Wasti" Weber and Peter Escher-Vetter provided great support on the computing side. Without Ludwig Braun, Erich Heucke, Ossi Reinwarth, Hermann Rentsch, Matthias Schulz, Lusia Soturczak, Roland Würländer and various other colleagues, data acquisition and evaluation would have been much more difficult, not to say impossible. Susan Braun-Clarke and Roger LeB. Hooke improved the language and part of the contents of this paper considerably. This work was funded by the Bavarian Climate Research Program BayFORKLIM and supported by the Federal Ministry for Education and Research and the State of Bavaria.

REFERENCES

Ambach, W., 1955: Über den nächtlichen Wärmeumsatz der gefrorenen Gletscheroberfläche. Arch.Met.Geoph.Biokl., Ser. A, 8(4), 411–426.

Arck, M., Escher-Vetter, H., 1997: Topoclimatological analysis of the reduction of the glaciers in the Zugspitz region, Bavaria. Z. Gletscherkd. Glazialgeol., 33(1), 57–72.

Arnold, N. S., Willis, I., Sharp, M., Richards, K., Lawson, W., 1996: A distributed surface energy-balance model for a small valley glacier. I. Development and testing for Haut Glacier d'Arolla, Valais, Switzerland. J. Glaciol., 42(140), 77–89.

Baker, D., Escher-Vetter, H., Moser, H., Oerter, H., Reinwarth, O., 1982: A glacier discharge model based on results from field studies of energy balance, water storage and flow. Hydr. aspects of alpine and high-mountain areas. IAHS Publ. No. 138, 103–112.

Bergmann, H., Reinwarth, O., 1976: Die Pegelstation Vernagtbach (Oetztaler Alpen). Planung, Bau und Meßergebnisse. Z. Gletscherkd. Glazialgeol., 12, 157–180.

Bolz, H., 1949: Die Abhängigkeit der infraroten Gegenstrahlung von der Bewölkung. Z. f. Met., 3, 97–100.

Braithwaite, R. J., Olesen, O. B., 1990: A simple energy-balance model to calculate ice ablation at the margin of the Greenland ice sheet. J. Glaciol., 36 (123), 222–228.

Braun, L.N., Escher-Vetter, H., 1996: Glacial discharge as affected by climate change. Intern. Symposion Interpraevent 1996 – Garmisch-Partenkirchen. Tagungspubl., 1, 65–74.

Brunt, D., 1932: Notes on radiation in the atmosphere. Quart. J. Royal Meteorol. Soc., 58, 389–420.

Brunt, D., 1944: Physical and Dynamical Meteorology. Cambridge University Press, 428 pp.

Escher-Vetter, H., 1980: Der Strahlungshaushalt des Vernagtferners als Basis der Energiehaushaltsberechnung zur Bestimmung der Schmelzwasserproduktion eines Alpengletschers. Münchner Universitäts-Schriften, Fachbereich Physik, Universität München – Met. Inst. Wiss. Mitt. Nr. 39, 115.

Escher-Vetter, H., 1985: Energy balance calculations for the ablation period 1982 at Vernagtferner, Oetztal Alps. Annals of Glaciology, 6, 158–160.

Escher-Vetter, H., Oerter, H., Zunke, D., Reinwarth, O., 1986: Modelling of the runoff from Vernagtferner (Oetztal Alps). Proc. Int. Symp."Glacier Mass-Balance, fluctuations and runoff", Academy of Sciences of the U.S.S.R., Soviet Geophysical Committee, 58, 65–69 (178–182).

Escher-Vetter, H., Reinwarth, O., 1994: Two decades of runoff measurements (1974 to 1993) at the Pegelstation Vernagtbach/Oetztal Alps. Z. Gletscherkd. Glazialgeol., 30, 53–98.

Finsterwalder, S., 1897: Der Vernagtferner. Wissenschaftliche Ergänzungshefte zur Zeitschrift des Deutschen und Österreichischen Alpenvereins 1, 5–96.

Fliri, F., 1975: Das Klima der Alpen im Raume von Tirol. Monographien zur Landeskunde Tirols. Folge I. Hrsg. A. Leidlmair u. F. Huter. Universitätsverlag Wagner, Innsbruck-München, 454 S.

Geiger, R., 1961: Das Klima der bodennahen Luftschicht. Friedr. Vieweg & Sohn, Braunschweig, 646 S.

Greuell, W., Böhm, R., 1998: 2 m temperatures along melting mid-latitude glaciers, and implications for the sensitivity of the mass balance to variations in temperature. J. Glaciol., 44(146), 9–20.

Heipke, C., Rentsch, H., Rentsch, M., Würländer, R., 1994: The digital orthophoto map Vernagtferner 1990. Z. Gletscherkd. Glazialgeol., 30, 109–117.

Hock, R., 1998: Modelling of glacier melt and discharge. Diss. ETH. No. 12430, Zürich, 126.
Hock, R., Noetzli, Ch., 1996: Areal melt and discharge modelling of Storglaciären, Sweden. Ann. Glaciol., 24, 211–217.
Hofinger, S., Kuhn, M., 1996: Reconstruction of the summer mass balance of Hintereisferner since 1953. Z. Gletscherkd. Glazialgeol., 32, 137–149.
Hoinkes, H., 1955: Über den Wärmehaushalt horizontaler Gletscherflächen in den Alpen. Meteorol. Abh. Bd. II, Heft 4, 53–62.
Hofmann, G., 1965: Zum Abbau der Schneedecke. Arch.Met.Geoph.Biokl., Ser. B, 13, 1–20.
Mader, M., Kaser, G., 1994: Application of a linear reservoir model to the discharge of a glacierized basin in the Silvretta mountains. Z. Gletscherkd. Glazialgeol., 30, 125–140.
Moser, H., Escher-Vetter, H., Oerter, H., Reinwarth, O., Zunke, D., 1986: Abfluss in und von Gletschern. GSF-Bericht 41/86, München, Teil I und II, 408, 147.
Nash, J.E., Sutcliffe, J. V., 1970: River flow forecasting through conceptual models. Part I – a discussion of principles. J. Hydrol., 10 (3), 282–290.
Oerlemans, J., 1993: A model for the surface balance of ice masses: part I. Alpine glaciers. Z. Gletscherkd. Glazialgeol., 27/28 (1991/1992), 63–83.
Oerlemans, J., Knap, W. H., 1998: A 1 year record of global radiation and albedo in the ablation zone of Morteratschgletscher, Switzerland. J. Glaciol, 44(147), 231–238.
Oerter, H., Baker, D., Moser, H., Reinwarth, O., 1981: Glacial-Hydrological Investigations at the Vernagtferner Glacier as a Basis for a Discharge Model. Nordic Hydr. 12 (4/5), 335–348.
Quervain, M. de., 1951: Zur Verdunstung der Schneedecke. Arch.Met.Geoph.Biokl., Ser. B, III, 47–64.
Reinwarth, O., Rentsch, H., 1994: Volume and mass balance of Vernagtferner/Oetztal Alps. Z. Gletscherkd. Glazialgeol., 30, 99–107.
Rohrer, M., 1992: Die Schneedecke im Schweizer Alpenraum und ihre Modellierung. Zürcher Geographische Schriften 49, 178 S.
Sauberer, F., Dirmhirn, I., 1958: Das Strahlungsklima – Klimatographie von Österreich, Wien. 196 S.
US Army Corps of Engineers, 1956: Snow Hydrology. US Department of Commerce, Office of Technical Services, PB 151 660, 437 pp.
Wagner, H. P., 1979: Strahlungshaushaltsuntersuchungen an einem Ostalpengletscher während der Hauptablationsperiode. Teil I: Kurzwellige Strahlung. Arch.Met.Geoph.Biokl., Ser.B, 27, 297–324.

Manuscript received 20 April 1999, revised 25 July 2000

Author's address: Heidi Escher-Vetter
Commission for Glaciology
Bavarian Academy of Sciences
Marstallplatz 8
D-80539 München, Germany